JCTC Journal of Chemical Theory and Computation

Gauge-Origin Independent Formulation and Implementation of Magneto-Optical Activity within Atomic-Orbital-Density Based Hartree−Fock and Kohn−Sham Response Theories

Thomas Kjærgaard* and Poul Jørgensen

The Lundbeck Foundation Center for Theoretical Chemistry, University of Aarhus, Langelandsgade 140, DK-8000 Århus C, Denmark

Andreas J. Thorvaldsen

Centre for Theoretical and Computational Chemistry, University of Tromsø, N-9037 Tromsø, Norway

Paweł Sałek

Department of Theoretical Chemistry, The Royal Institute of Technology SE-10691 Stockholm, Sweden

Sonia Coriani

Dipartimento di Scienze Chimiche, Università degli Studi di Trieste via L. Giorgieri 1, I-34127 Trieste, Italy, and Centre for Theoretical and Computational Chemistry, University of Oslo, P.O. Box 1033 Blindern, N-0315 Oslo, Norway

Received April 6, 2009

Abstract: A Lagrangian approach has been used to derive gauge-origin independent expressions for two properties that rationalize magneto-optical activity, namely the Verdet constant $V(\omega)$ of the Faraday effect and the $\mathscr{B}$ term of magnetic circular dichroism. The approach is expressed in terms of an atomic-orbital density-matrix based formulation of response theory and use London atomic orbitals to parametrize the magnetic field dependence. It yields a computational procedure which is both gauge-origin independent and suitable for linear-scaling at the level of time-dependent Hartree−Fock and density functional theory. The formulation includes a modified preconditioned conjugated gradient algorithm, which projects out the excited state component from the solution to the linear response equation. This is required when solving one of the response equations for the determination of the $\mathscr{B}$ term and divergence is encountered if this component is not projected out. Illustrative results are reported for the Verdet constant of H_2, HF, CO, N_2O, and $CH_3CH_2CH_3$ and for the $\mathscr{B}$ term of pyrimidine, phosphabenzene, and pyridine. The results are benchmarked against gauge-origin independent CCSD values.

1. Introduction

It is well-known that a static magnetic field applied in the direction of propagation of linearly polarized light impinging on matter induces an optical response, irrespective of the chirality of the sample. What is observed is either a rotation of the plane of polarization of the emerging light in the transparent regions of the sample (magneto-optical rotation, MOR, or magnetic circular birefringence MCB, also known as Faraday effect) or an ellipticity or dichroism in the

* To whom correspondence should be addressed. E-mail: tkjaergaard@chem.au.dk.

10.1021/ct9001625 CCC: $40.75
Published on Web 07/06/2009

absorptive regions (magnetic circular dichroism, MCD). Both phenomena are collectively referred to as magneto-optical activity (MOA) and originate from a differential interaction of the sample with the right and left circularly polarized components of the plane-polarized light because of the presence of the perturbing magnetic field. For MOR the magnetic field causes the two components to propagate with different velocities, hereby, the rotation; for MCD the two components are absorbed to a different extent and the ellipticity occurs.[1–6] Magnetic optical activity has turned out to become a valuable spectroscopic tool, in particular for studying the structure and electronic configurations of inorganic complexes, porphyrins, heme, and nonheme proteins.[7–11]

MOR is conventionally rationalized in terms of the so-called Verdet constant,[12] which according to molecular perturbation theory, is connected to the dipole−dipole-magnetic dipole hyperpolarizability.[3–5] The theoretical determination of the Verdet constant has been used as a probe of the electronic structure of the sample,[13,14] to test the accuracy of new methods in computing high-order molecular properties,[15–19] and even as source of information on structure−property relationships for organic molecules, which might be of importance in designing materials with outstanding magneto-optical properties.[14]

The induced dichroism is employed in the well-known MCD spectroscopy,[20–23] which is widely used in inorganic chemistry, often with focus on the elucidation of the electronic structure of porphyrins and phthalocyanines,[9,10] and in biological chemistry,[11,24–26] for instance as a powerful probe of metalloenzyme active-sites.[24] MCD spectra are traditionally rationalized in terms of three magnetic rotatory strengths, known as the Faraday $\mathscr{A}$, $\mathscr{B}$, and $\mathscr{C}$ terms.[5,6,27–31] The $\mathscr{A}$ term only contributes if either the ground or the excited state is degenerate, and the $\mathscr{C}$ term only contributes if the ground state is degenerate. The $\mathscr{B}$ term contributes irrespective of the degeneracy of the ground and final excited states and therefore describes the MCD spectrum of an electronic transition in a molecule without electronic state degeneracies. Even though it may be questioned whether it is necessary to separate the evaluation (and interpretation) of the MCD into $\mathscr{A}$ and $\mathscr{B}$ terms,[32] the generally low symmetry of large organic molecules justifies the focus on the $\mathscr{B}$ term as the $\mathscr{A}$ and $\mathscr{C}$ terms vanish in the absence of an axis of 3-fold or higher symmetry.[4,22,23,33] After a few decades of relatively scarce attention, the computational determination of the MCD parameters and spectra is experiencing a renewed interest, both from the methodological and the applicative point of view, with a steady increase in the number of publications, in particular during the last five years.[17,32,34–46]

A common difficulty in the calculation of magnetic properties is that approximate methods do not automatically guarantee gauge-origin independence of the results. The computed results might therefore end up depending on the origin of the vector potential. Only in the limit of a complete basis set do they become gauge-origin independent. A large basis set can then be expected to yield approximate gauge invariance, but its use is not always a viable technique, in particular for very large systems.

For systems belonging to certain symmetry groups (e.g., atomic and centro-symmetric systems) the Verdet constant is known to be automatically origin independent, and it can be straightforwardly obtained from the dipole, dipole, magnetic dipole quadratic response function. Such an approach has been extensively used in the past at various levels of theory, from Hartree−Fock to coupled cluster and for various systems.[14–16,47–49] For atoms, Cauchy expansions and linear response function approaches have also been employed.[50,51]

The first gauge-origin independent approach to compute Verdet constants was proposed by Coriani et al.[17] within coupled cluster singles and doubles (CCSD) response theory and made use of London atomic orbitals (LAO),[52–54] which introduce local gauge-origins to define the vector potential of the external magnetic field. A similar strategy was adopted a few years later by Banerjee and co-workers[18,19] at the time-dependent (TD) density functional theory (DFT) level, in a molecular orbital-based formulation.

Concerning the MCD strengths, early methods to calculate the $\mathscr{B}$ term have in general been based on sum-overstates (SOS) procedures,[55–61] often at a semiempirical level. Seth et al.[41] presented a $\mathscr{B}$-SOS method at the TD-DFT level of theory in a molecular orbital based formulation. Any SOS method suffers from errors caused by truncations in the number of excitations that are considered.

The SOS method is gauge-origin dependent, like any numerical calculation which is forced to use an incomplete basis set of field-free eigenfunctions.[33,62] Caldwell and Eyring[4,62] have shown that the error introduced by using a limited basis set is minimized at the center of the charge density, and several authors have reported that the location of the origin within the framework of the molecule yields qualitatively correct results.[63,64]

In ref 34 the $\mathscr{B}$ term was evaluated, for naturally gauge-origin independent molecules,[33] as the first residue of the frequency dependent quadratic response functions.[34] The method can be considered superior to the SOS procedure, but no general solution for the treatment of the gauge-origin problem was proposed.[34] Note that the usual interpretation of MCD in terms of magnetic mixing is lost in such an approach, as reference to intermediate states is avoided. An extension of the approach to include solvent effects was proposed in ref 37.

Several papers have recently appeared on the computational simulation of MCD spectra,[17,32,35–46,65] including $\mathscr{A}$, $\mathscr{B}$, and $\mathscr{C}$ terms. We bring attention in particular to the novel complex polarization approach of ref 38 and the rather similar approach based on the imaginary part of the Verdet constant using damped time-dependent density functional theory in ref 44. In the latter, in particular, the use of London orbitals in the determination of the damped Verdet constant allows to remove the gauge-origin dependence problem at the DFT level. Ref 42 applies a magnetically perturbed TD-DFT[66] to calculate the $\mathscr{B}$ term of MCD and describes both a SOS approach and a direct approach. The direct approach is similar to the approach presented by Coriani et al.[34]

The use of London orbitals to remove the gauge-origin dependence in the calculation of the $\mathscr{B}$ term was first proposed in 1972 by Seaman and Linderberg[67] and implemented within a finite perturbation (FP) method. Coriani et al. presented in ref.,[17] together with the gauge-independent expression for the Verdet constant, also a gauge-origin independent formulation of the $\mathscr{B}$ term at the CCSD level using LAOs. The method was later applied to a number of selected molecules[36] and gave $\mathscr{B}$ terms of a high quality, but it is hampered by its computational cost and is limited to molecules of the size of pyrimidine and phosphabenzene.

The Hartree−Fock approximation may be used to calculate $\mathscr{B}$ term of larger molecules, but early studies showed that the Hartree−Fock method may not even produce the correct sign for the $\mathscr{B}$ term.[34,37] It was also concluded that electron correlation effects are, as for other optical properties, important for determining the $\mathscr{B}$ term.

One way to efficiently include electron correlation effects for large molecules is via density functional theory (DFT). DFT is known to give reasonable accuracy at a low computational cost,[68−70] and recent linear scaling implementations make Kohn−Sham DFT (along with Hartree−Fock) applicable to molecules consisting of more than 1000 atoms. In ref 71, for instance, linear scaling of the DFT Kohn−Sham (KS) method has been obtained by a reformulation in a orthogonal atomic orbital (OAO) basis, the Löwdin basis. The orthogonal OAO basis is advantageous to use to describe local phenomena such as the Coulomb cusp. In addition to exploiting locality the Löwdin orthogonalization reduces the condition number of the KS matrix, a very attractive feature when solving the response equations of DFT.

The locality of the orbitals makes matrices sparse, and with the use of sparse matrix algebra,[72] it is possible to avoid the high scaling of the standard electronic structure models and achieve linear scaling. The use of the method requires an efficient and linear-scaling transformation from the AO basis to the Löwdin OAO basis, which has been developed and implemented by Jansík et al.[73]

Coriani et al.[74] addressed the problem of the computation of molecular properties at a linear cost and used the Löwdin OAO basis to obtain an atomic orbital based response solver which allows for the linear scaling calculation of excitation energies, transition strengths and frequency dependent linear response functions (polarizabilities) at the Hartree−Fock and Kohn−Sham (TD-DFT) levels of theory. The method has been recently extended to the general frequency-dependent quadratic response function and its residues by Kjærgaard et al.[75]

We here present a gauge-origin independent formulation of the Verdet constant and of the $\mathscr{B}$ terms of MCD within the linear scaling framework of Hartree−Fock/Kohn−Sham-DFT response theory of ref 74. Gauge-origin independent analytic expressions for the two MOA properties are found using a Lagrangian technique, where each property is expressed as a total derivative, with respect to the strength of the external magnetic field, of an appropriate linear-response functional whose magnetic field dependence is parametrized by means of LAOs. By choosing, as starting expressions, lower-order property AO-based expressions,[74,76] we automatically obtain working equations which are prone to linear scaling for sufficiently sparse matrices. The atomic orbital basis, in addition to guaranteeing scalability and ease of parallelization, also represents a "natural" framework for deriving property expressions for perturbation dependent basis sets.

The procedure adopted here is presented in more general terms in ref 77, where the focus lies on geometrical derivatives. It also bears similarities with Furche and co-workers'[78,79] conventional molecular-orbital formulation of excited state gradients and vibrational Raman intensities using time-dependent density functional theory. Geometric and magnetic perturbations can in fact be treated on the same footing, as involving different types of perturbation-dependent basis sets. Similarities may also be found with the method presented by Thorvaldsen et al.[80] for the calculation at the Kohn−Sham level of molecular properties to arbitrary order, in which the quasienergy and Lagrangian formalisms are combined to derive response functions by differentiation of the quasienergy derivative Lagrangian using the elements of the AO density matrix as variational parameters, and which was implemented, at the Hartree−Fock level only, to obtain for instance gauge-origin independent values of the mixed electric and magnetic first hyperpolarizability entering the temperature-independent term of Buckingham's birefringence.[81] Such quantity is somewhat connected to the Verdet constant, as discussed for instance in refs 51 and 82.

When London orbitals are not used we recover, as a subset of our derivation, the standard expression for the quadratic response function $\langle\langle \hat{\mu}_\alpha; \hat{\mu}_\beta, \hat{m}_\gamma \rangle\rangle_{\omega,0}$ and its residues, with $\hat{\mu}$ being the electric dipole operator and $\hat{\mathrm{m}}$ the magnetic dipole, that is, the standard quadratic response expressions for the Verdet constant $V(\omega)$ and the $\mathscr{B}$ term of MCD.[34] Note that when evaluating the $\mathscr{B}$ term, we also ensure that unphysical divergencies related to singularities in the response equations are projected out.

The method is mainly benchmarked against new and previous CCSD results.[17,36] This is expected to be of particular relevance for MCD, as it will increase the reliability of these calculations for the assignment of excited states for large molecules. The CCSD study of Kjærgaard et al.[36] showed that Kohn−Sham DFT calculations cannot directly be benchmarked against experimental results because of the cancellation between positive and negative contributions.

The paper is organized as follows. In the Theory section, we define first the key quantities which constitute the formal background of our derivation. We then present the Lagrange method for the properties of interest. In the Results and Discussion section, we report pilot numerical results for a few selected cases, addressing both gauge-origin independence and convergence issues.

2. Theory

2.1. Definition of the MOA Properties: Derivative Expressions of $V(\omega)$ and $\mathscr{B}(n \rightarrow j)$. Following the approach of Coriani et al.,[17] we define the Verdet constant $V(\omega)$ of the Faraday effect as[5]

$$V(\omega) = \left\langle \left(\frac{\mathrm{d}\phi}{\mathrm{d}B_z} \right)_{\boldsymbol{B}=0} \right\rangle = \omega C \epsilon_{\alpha\beta\gamma} \left(\frac{\mathrm{d}\alpha'_{\alpha\beta}(-\omega;\omega)}{\mathrm{d}B_\gamma} \right)_{\boldsymbol{B}=0} = C\omega\epsilon_{\alpha\beta\gamma}\alpha'^{(m)}_{\alpha,\beta,\gamma} \quad (1)$$

where ϕ is the optical rotation, $\alpha'_{\alpha\beta}(-\omega;\omega)$ is the (magnetic-field perturbed) antisymmetric electric dipole polarizability (the imaginary part of the complex polarizability $\tilde{\alpha}_{\alpha\beta}(-\omega;\omega)$), ω is the frequency of the incident polarized light and $\varepsilon_{\alpha\beta\gamma}$ is the Levi−Civita tensor.[3] C is a collection of fundamental constants, $C = (1)/(12)\mu_0 cN$, where c is the speed of light in vacuo, μ_0 is the permeability of free space, and N is the number density. B_z is the z Cartesian component of the magnetic field induction. Note that this expression only holds for an isotropic sample of closed shell molecules, otherwise an additional temperature dependent term would appear.[3]

Similarly, we identify the Faraday $\mathscr{B}(n \rightarrow j)$ from the derivative of a (magnetic-field perturbed) one-photon dipole transition strength $S^{\alpha\beta}_{nj} = \langle n|\hat{\mu}_\alpha|j\rangle\langle j|\hat{\mu}_\beta|n\rangle \equiv \mu^{nj}_\alpha \mu^{jn}_\beta$

$$\mathscr{B}(n \rightarrow j) = \frac{1}{2}\epsilon_{\alpha\beta\gamma}\mathscr{I}\left(\frac{\mathrm{d}S^{\alpha\beta}_{nj}}{\mathrm{d}B_\gamma} \right)_{\boldsymbol{B}=0} \quad (2)$$

where $|n\rangle$ is the ground state.[17,67]

We mention here that a derivative expression was recently proposed by Seth and co-workers[39] also for the $\boldsymbol{A}$ term

$$\mathscr{A}(n \rightarrow j) = -\frac{1}{2}\epsilon_{\alpha\beta\gamma}\sum_r \left(\frac{\partial \omega_{j_r}}{\partial B_\gamma} \right)_{\boldsymbol{B}=0} \mathscr{I}(\mu^{nj_r}_\alpha \mu^{j_r n}_\beta) \quad (3)$$

where ω_{j_r} is the excitation frequency from the ground state to the degenerate excited state $|j_r\rangle$, with r running on the number of degenerate states. We defer the calculation of the $\mathscr{A}$ term to a later publication.

According to the definitions above, the two MOA properties are hence magnetic-field derivatives of quantities that can be obtained, within response theory,[83] from the so-called linear response function. It is well-known that the electric dipole polarizability corresponds to the linear response function

$$\alpha_{\alpha\beta}(-\omega;\omega) = -\langle\langle \hat{\mu}_\alpha;\hat{\mu}_\beta \rangle\rangle_\omega \quad (4)$$

where μ_α is the α Cartesian component of the electric dipole operator. Similarly, the transition strength is obtained from the residue of the linear response function

$$S^{\alpha\beta}_{nj} = \lim_{\omega\rightarrow\omega_j}(\omega - \omega_j)\langle\langle \hat{\mu}_\alpha;\hat{\mu}_\beta \rangle\rangle_\omega \quad (5)$$

The definitions above allow us to derive gauge-origin independent expressions by setting up a two-step approach that starts from the analytic expressions for the linear response functions in an AO based framework (section 2.2) and where the magnetic field dependence in the linear response quantities is parametrized through the LAOs (section 2.3). By exploiting a Lagrangian approach, we can moreover take advantage of the $2n + 1$ and $2n + 2$ rules to avoid computing the responses to the magnetic field of the linear response vectors and/or excitation vectors, and of the variational parameters involved in the wavefuntion/density optimization (section 2.4).

Table 1. Explicit Expressions for the Various Vectors, Matrices and Super-Matrices Entering the Linear Response Function in the Hartree-Fock Case[a]

$E^{[1]}_m$	=	$\mathrm{Tr}\mathbf{O}^\dagger_m[\mathbf{F},\mathbf{S}]_\mathrm{D}$
$B^{[1]}_m$	=	$\mathrm{Tr}\mathbf{O}^\dagger_m[\mathbf{B},\mathbf{S}]_\mathrm{D}$
$A^{[1]}_m$	=	$\mathrm{Tr}\mathbf{O}^\dagger_m[\mathbf{A},\mathbf{S}]_\mathrm{D}$
$E^{[2]}_{mn}$	=	$\mathrm{Tr}\mathbf{F}[[\mathbf{O}_n,\mathbf{D}]_\mathrm{S},\mathbf{O}^\dagger_m]_\mathrm{S} + \mathrm{Tr}\mathbf{G}([\mathbf{O}_n,\mathbf{D}]_\mathrm{S})[\mathbf{D},\mathbf{O}^\dagger_m]_\mathrm{S}$
$S^{[2]}_{mn}$	=	$\mathrm{Tr}\mathbf{O}^\dagger_m\mathbf{S}[\mathbf{D},\mathbf{O}_n]_\mathrm{S}\mathbf{S}$
$E^{[3]}_{mnj}$	=	$\mathrm{Tr}\mathbf{F}[[\mathbf{O}_n,[\mathbf{O}_j,\mathbf{D}]_\mathrm{S}],\mathbf{O}^\dagger_m]_\mathrm{S} + \mathrm{Tr}\mathbf{G}([\mathbf{O}_j,\mathbf{D}]_\mathrm{S})[[\mathbf{O}_n,\mathbf{D}]_\mathrm{S},\mathbf{O}^\dagger_m]_\mathrm{S} + \mathrm{Tr}\mathbf{G}([\mathbf{O}_n,\mathbf{D}]_\mathrm{S})[[\mathbf{O}_j,\mathbf{D}]_\mathrm{S},\mathbf{O}^\dagger_m]_\mathrm{S} + \mathrm{Tr}\mathbf{G}([\mathbf{O}_n,[\mathbf{O}_j,\mathbf{D}]_\mathrm{S}]_\mathrm{S})[\mathbf{D},\mathbf{O}^\dagger_m]_\mathrm{S}$
$S^{[3]}_{mnj}$	=	$-\mathrm{Tr}\ \mathbf{O}^\dagger_m\mathbf{S}[\mathbf{O}_n,[\mathbf{D},\mathbf{O}_j]_\mathrm{S}]_\mathrm{S}\mathbf{S}$
$B^{[2]}_{mj}$	=	$-\mathrm{Tr}\mathbf{B}[[\mathbf{O}_j,\mathbf{D}]_\mathrm{S},\mathbf{O}^\dagger_m]_\mathrm{S}$
$A^{[2]}_{mj}$	=	$\mathrm{Tr}\mathbf{A}^\dagger[[\mathbf{O}_j,\mathbf{D}]_\mathrm{S},\mathbf{O}^\dagger_m]_\mathrm{S}$

[a] The superscript refers to the order of differentiation with respect to the variational parameters $\mathbf{X}$ in the density matrix. Note that $(\partial\mathbf{D}(\mathbf{X}))/(\partial X_j) = -[\mathbf{O}_j,\mathbf{D}]_\mathrm{S}$.

2.2. AO-Based Linear Response Theory. The linear response function is the first-order term in the perturbative expansion, with respect to a (periodic) perturbation, $\hat{V}^t = \int_{-\infty}^{+\infty}\hat{V}^\omega \exp(-i\omega t)\mathrm{d}\omega$, of the time-dependent expectation value of an observable represented by the time-independent operator $\hat{A}$

$$\langle A\rangle(t) = \langle A\rangle_0 + \int \langle\langle \hat{A};\hat{V}^\omega \rangle\rangle_\omega \exp(-i\omega t)\mathrm{d}\omega + \ldots \quad (6)$$

where $\langle\langle \hat{A};\hat{V}^\omega \rangle\rangle_\omega$ is the linear response function in the frequency domain. The linear response function (LRF) is required for the calculation of the Verdet constant, according to eqs 4 and 1.

Assuming implicit summation over repeated indices and introducing the symbol $\hat{B}$ in place of $\hat{V}^\omega$, the linear response function (LRF) expression according to the AO parametrization of response theory of refs 74 and 76 is

$$\langle\langle \hat{A};\hat{B} \rangle\rangle_\omega = -\boldsymbol{A}^{[1]\dagger}\boldsymbol{b}^\omega \equiv -\mathrm{Tr}\{\mathbf{A}^{[1]\dagger}\mathbf{b}^\omega\} \quad (7)$$

where the elements b^ω_m of the response vector $\boldsymbol{b}^\omega$ are obtained from the solution of the linear response equation

$$(\boldsymbol{E}^{[2]} - \omega\boldsymbol{S}^{[2]})\boldsymbol{b}^\omega = \boldsymbol{B}^{[1]} \quad (8)$$

Above, $\boldsymbol{A}^{[1]}$ is the so-called *property gradient* relative to the $\hat{A}$ operator, whereas $\boldsymbol{B}^{[1]}$ is the *property gradient* relative to the external perturbation described by V^ω ($\equiv \hat{B}$) and $\boldsymbol{E}^{[2]}$ and $\boldsymbol{S}^{[2]}$ are the generalized (RPA) electronic Hessian and metric matrices in the AO basis.[76] Their explicit expressions are collected in Table 1. Note that the elements of $\boldsymbol{E}^{[2]}$ are here defined with sign opposite compared to the one given in eq 65 of ref 76. The reasons for such a sign change are explained in detail in ref 75.

Note also the use of italic boldface characters to indicate vectors and matrices in a so-called *supermatrix* notation,[83,84] and of roman bold face characters to indicate true matrices in the AO space (of dimension N^2_AO). According to the supermatrix notation, an AO matrix element, for instance the $B^{[1]}_{\mu\nu}$ element of the property gradient matrix $\mathbf{B}^{[1]}$, corresponds to the element $B^{[1]}_m$ of a property gradient *(column) vector* $\boldsymbol{B}^{[1]}$, where m is ordered such that the

excitations precede the de-excitations. As a rule of thumb we can go from the (element-wise) supermatrix notation to the true matrix representation in the AO basis using

$$M_j = \mathrm{Tr}\mathbf{O}_j^\dagger \mathbf{M} = \mathrm{Tr}\mathbf{O}_j \mathbf{M}^\dagger \tag{9}$$

which associates the j element of vector $\boldsymbol{M}$ with the $M_{\mu\nu}$ element of the matrix $\mathbf{M}$ in the AO basis. The operators $\mathbf{O}_j^\dagger$ and $\mathbf{O}_j$ are defined in ref 76 to be

$$\mathbf{O}_j = \begin{cases} \mathbf{E}_{\mu\nu} & j > 0 \\ \mathbf{E}_{\nu\mu} & j < 0 \end{cases} \tag{10}$$

where $\mathbf{E}_{\mu\nu}$ is a unit matrix with elements given by

$$[\mathbf{E}_{\mu\nu}]_{\rho\sigma} = \delta_{\mu\rho}\delta_{\nu\sigma} \tag{11}$$

We also introduce the expansions

$$\boldsymbol{b}^\omega = \sum_m b_m^\omega \mathbf{O}_m; \qquad \boldsymbol{b}^{\omega\dagger} = \sum_m b_m^\omega \mathbf{O}_m^\dagger \tag{12}$$

where the first vector is a column vector, and the second one is a row vector. In the AO basis their matrix representations will be indicated as $\mathbf{b}^\omega$ and $\mathbf{b}^{\omega\dagger}$, respectively.

As indicated in Table 1, the property gradients and generalized Hessian and metric contain matrix products of integral matrices in the AO space, namely the AO overlap matrix $\mathbf{S}$, the AO integral matrices $\mathbf{A}$ and $\mathbf{B}$ for the $\hat{A}$ and $\hat{B}$ operators, respectively, the AO density matrix $\mathbf{D}$, the Fock

$$\mathbf{F} = \mathbf{h} + \mathbf{G}^{\mathrm{HF}}(\mathbf{D}) \tag{13}$$

or Kohn−Sham[75]

$$\mathbf{F} = \mathbf{h} + \mathbf{G}^{\mathrm{HF}}(\mathbf{D}) + \mathbf{F}^{\mathrm{xc}} \tag{14}$$

matrices, where

$$G_{\mu\nu}^{\mathrm{HF}}(\mathbf{D}) = \sum_{\rho\sigma} D_{\sigma\rho}\,[\mathscr{g}_{\mu\nu\rho\sigma} - w_x \mathscr{g}_{\mu\sigma\rho\nu}] \tag{15}$$

The scaling factor w_x is equal to 1 for Hartree−Fock; in the DFT case it is only nonzero for hybrid theories. The last term in eq 14 is the derivative of the exchange-correlation functional $E_{\mathrm{xc}}[\rho]$, which depends on the density ρ

$$F_{\mu\nu}^{\mathrm{xc}} = \frac{\partial E_{\mathrm{xc}}[\rho]}{\partial D_{\nu\mu}} \tag{16}$$

Expressing the density ρ in the AO basis as

$$\rho(\mathbf{r}) = \sum_{\mu\nu} \chi_\mu^*(\mathbf{r})\chi_\nu(\mathbf{r}) D_{\nu\mu} = \sum_{\mu\nu} \Omega_{\mu\nu}(\mathbf{r}) D_{\nu\mu} \tag{17}$$

where $\Omega_{\mu\nu}(\mathbf{r}) = \chi_\mu^*(\mathbf{r})\chi_\nu(\mathbf{r})$ is the overlap distribution, and introducing the exchange-correlation potential

$$v_{\mathrm{xc}}(\mathbf{r}) = \frac{\delta E_{\mathrm{xc}}[\rho]}{\delta\rho(\mathbf{r})} \tag{18}$$

it is seen that

$$F_{\mu\nu}^{\mathrm{xc}} = \int \frac{\delta E_{\mathrm{xc}}[\rho]}{\delta\rho(\mathbf{r})} \frac{\partial\rho(\mathbf{r})}{\partial D_{\nu\mu}} \mathrm{d}\mathbf{r} = \int v_{\mathrm{xc}}(\mathbf{r})\Omega_{\mu\nu}(\mathbf{r})\mathrm{d}\mathbf{r} \tag{19}$$

is the AO matrix representation of the exchange-correlation potential. Within the exponential parametrization of the density matrix, density matrices are related through the transformation

$$\mathbf{D}(\mathbf{X}) = \exp(-\mathbf{XS})\mathbf{D}\exp(\mathbf{SX}) = \mathbf{D} + [\mathbf{D},\mathbf{X}]_{\mathbf{S}} + \frac{1}{2}[[\mathbf{D},\mathbf{X}]_{\mathbf{S}},\mathbf{X}]_{\mathbf{S}} + \ldots \tag{20}$$

where $\mathbf{X}$ is an anti-Hermitian matrix that contains the variational parameters, with the redundant parameters projected out

$$\mathbf{X} = \mathscr{P}(\mathbf{X}) \equiv \mathbf{P}_{\mathrm{o}}\mathbf{X}\mathbf{P}_{\mathrm{v}}^{\mathrm{T}} + \mathbf{P}_{\mathrm{v}}\mathbf{X}\mathbf{P}_{\mathrm{o}}^{\mathrm{T}} \tag{21}$$

$\mathbf{P}_{\mathrm{o}}$ and $\mathbf{P}_{\mathrm{v}}$ are projectors onto the occupied and virtual orbital spaces, respectively

$$\mathbf{P}_{\mathrm{o}} = \mathbf{DS} \tag{22}$$

$$\mathbf{P}_{\mathrm{v}} = \mathbf{I} - \mathbf{DS} \tag{23}$$

fulfilling the idempotency ($\mathbf{P}_{\mathrm{o}}^2 = \mathbf{P}_{\mathrm{o}}$ and $\mathbf{P}_{\mathrm{v}}^2 = \mathbf{P}_{\mathrm{v}}$) and orthogonality relations ($\mathbf{P}_{\mathrm{o}}\mathbf{P}_{\mathrm{v}} = \mathbf{P}_{\mathrm{v}}\mathbf{P}_{\mathrm{o}} = 0$ and $\mathbf{P}_{\mathrm{o}}^{\mathrm{T}}\mathbf{S}\mathbf{P}_{\mathrm{v}} = \mathbf{P}_{\mathrm{v}}^{\mathrm{T}}\mathbf{S}\mathbf{P}_{\mathrm{o}} = 0$). We have used the so-called S-commutator

$$[\mathbf{D},\mathbf{X}]_{\mathbf{S}} = \mathbf{DSX} - \mathbf{XSD} \tag{24}$$

For later convenience we also introduce a generalized M commutator as

$$[\mathbf{L},\mathbf{N}]_{\mathbf{M}} = \mathbf{LMN} - \mathbf{NML} \tag{25}$$

The linear response function has poles whenever the frequency ω is equal to an excitation energy ω_f. The excitation energies ω_f and excitation vectors $\boldsymbol{b}^f$ (matrices $\mathbf{b}^f$) are obtained from the solution of the generalized eigenvalue equation

$$(\boldsymbol{E}^{[2]} - \omega_f \boldsymbol{S}^{[2]})\boldsymbol{b}^f = 0 \tag{26}$$

The excited state vector is normalized over the generalized metric matrix $\boldsymbol{S}^{[2]}$, that is

$$\boldsymbol{b}^{f\dagger}\boldsymbol{S}^{[2]}\boldsymbol{b}^f = 1 \tag{27}$$

We note that $\boldsymbol{S}^{[2]}$ is *not* positive definite.

To calculate the Faraday $\mathscr{B}$ term, the residue of the linear response function is required (see eqs 2 and 5). The expression for the residue of the linear response function is, according to the AO parametrization of response theory, given by[74]

$$\lim_{\omega\to\omega_f}(\omega - \omega_f)\langle\langle A;B\rangle\rangle_\omega = (\boldsymbol{A}^{[1]\dagger}\boldsymbol{b}^f)(\boldsymbol{b}^{f\dagger}\boldsymbol{B}^{[1]}) = \mathrm{Tr}\{\mathbf{A}^{[1]\dagger}\mathbf{b}^f\}\mathrm{Tr}\{\mathbf{b}^{f\dagger}\mathbf{B}^{[1]}\} \tag{28}$$

2.3. Parametrization of the Magnetic Field Dependence: The LAO Basis and the (Differentiated) Integral Matrices in the LAO Basis. London atomic orbitals are used to parametrize the magnetic field dependence of the properties

to be differentiated. For a given atomic orbital $\chi(\mathbf{r}_M)$ centered on the nucleus M at position $\mathbf{R}_M$, the London orbital[52] is defined

$$\omega_\mu(\mathbf{r}_M, \mathbf{B}) = \exp\left\{-\frac{i}{2}\mathbf{B}\cdot[(\mathbf{R}_M - \mathbf{O})\times\mathbf{r}]\right\}\chi_\mu(\mathbf{r}_M) \tag{29}$$

where $\chi_\mu(\mathbf{r}_M)$ is a standard atomic orbital. Hence, the LAO depends parametrically on the magnetic field $\mathbf{B}$, the gauge origin $\mathbf{O}$ and the orbital position $\mathbf{R}_M$.

The LAOs introduce a magnetic field dependence in the integral matrices through exponential factors modifying the operators

$$O_{\mu\nu}(\mathbf{B}) = \langle\mu|\exp\left(\frac{i}{2}\mathbf{B}\cdot\mathbf{R}_{MN}\times\mathbf{r}\right)\hat{O}|\nu\rangle \tag{30}$$

where $\hat{O}$ is any one-electron operator or a Cartesian component operator, and

$$g_{\mu\nu\rho\sigma}(\mathbf{B}) = \langle\mu\nu|\exp\left\{\frac{i}{2}\mathbf{B}\cdot(\mathbf{R}_{MN}\times\mathbf{r}_1 + \mathbf{R}_{RS}\times\mathbf{r}_2)\right\}r_{12}^{-1}|\rho\sigma\rangle \tag{31}$$

are the magnetic-field dependent two-electron integrals; $\mathbf{R}_{MN} = \mathbf{R}_M - \mathbf{R}_N$ is the distance vector between nucleus M and nucleus N. Note that $\chi_\nu(\mathbf{r}_N)$, $\chi_\rho(\mathbf{r}_R)$, and $\chi_\sigma(\mathbf{r}_S)$ are centered at $\mathbf{R}_N$, $\mathbf{R}_R$, and $\mathbf{R}_S$, respectively. The one-electron operators of relevance in our specific case are the identity operator (for the overlap matrix integrals), the electric dipole operator ($\hat{O} = \mu_x,\mu_y,\mu_z$), and the one-electron Hamiltonian h_N

$$h_N(\mathbf{r};\mathbf{B},\mathbf{m}) = \frac{1}{2}\pi_N^2 - \sum_k \frac{Z_k}{|\mathbf{r} - \mathbf{R}_k|} \tag{32}$$

$$\pi_N = -i\nabla + \frac{1}{2}\mathbf{B}\times\mathbf{r}_N + \alpha^2\sum_K \frac{\mathbf{m}_K\times\mathbf{r}_K}{r_K^3} \tag{33}$$

The second term in the kinetic momentum operator π_N represents an externally applied uniform magnetic field $\mathbf{B}$, and the third term represents the field from a nuclear point magnetic moment $\mathbf{m}_K$, where α is the fine structure constant. The integrals over LAOs have been shown to be origin independent.[53]

Explicit expressions for the differentiated overlap, electric dipole, and Hamilton operator matrices (including the electron repulsion) have previously been reported,[53,54] and we refer the interested reader to the original papers. In the DFT case, however, we need to consider the modifications resulting from the use of LAOs in the exchange-correlation contribution $\mathbf{F}^{xc}$ to the Kohn−Sham matrix in eq 14 and in the exchange correlation contribution $\mathbf{G}^{xc}(\mathbf{M})$ to the (generalized) Kohn−Sham Hessian $\boldsymbol{E}^{[2]}$ (see Table 1 and refs 75 and 76), and the resulting magnetic field derivatives. The evaluation of these terms is described in details in Appendix B.

For completeness, we report here the final result, which has been derived under the assumption that the exchange correlation energy is the integral over all space of some functional $f = f[\rho,\xi]$, which depends on the density ρ and on the norm of the density gradient $\xi = |\nabla\rho|$. The exchange correlation contribution to the Kohn−Sham matrix is

$$F_{\mu\nu}^{xc} = \int\frac{\partial f}{\partial\rho}\Omega_{\mu\nu}(\mathbf{r})d\mathbf{r} + \int\frac{\partial f}{\partial\xi}\frac{\partial\xi}{\partial\nabla\rho}\nabla\Omega_{\mu\nu}(\mathbf{r})d\mathbf{r} \tag{34}$$

and its magnetic field derivative (see ref 85) becomes

$$\left.\frac{\partial F_{\mu\nu}^{xc}}{\partial B}\right|_{B=0} = \frac{i}{2}\int(\mathbf{R}_{MN}\times\mathbf{r})\left[\frac{\partial f}{\partial\rho(\mathbf{r})}\Omega_{\mu\nu}(\mathbf{r}) + \frac{\partial f}{\partial\xi}\frac{\nabla\rho(\mathbf{r})}{\xi}\nabla\Omega_{\mu\nu}(\mathbf{r})\right]d\mathbf{r} + \frac{i}{2}\int\left(\mathbf{R}_{MN}\times\frac{\nabla\rho(\mathbf{r})}{\xi}\right)\frac{\partial f}{\partial\xi}\Omega_{\mu\nu}(\mathbf{r})d\mathbf{r} \tag{35}$$

For the exchange-correlation contribution to the (generalized) Kohn−Sham Hessian, we obtain

$$G_{\mu\nu}^{xc}(\mathbf{M}) = \sum_{\rho\sigma}M_{\sigma\rho}\int\left[\frac{\partial^2 f}{\partial\rho^2}\Omega_{\mu\nu}\Omega_{\rho\sigma} + \frac{\partial^2 f}{\partial\rho\partial\xi}\left(\Omega_{\mu\nu}\frac{\nabla\rho}{\xi}\nabla\Omega_{\rho\sigma} + \Omega_{\rho\sigma}\frac{\nabla\rho}{\xi}\nabla\Omega_{\mu\nu}\right)\right]d\mathbf{r} + \sum_{\rho\sigma}M_{\sigma\rho}\int\frac{\partial^2 f}{\partial\xi^2}\left(\frac{\nabla\rho}{\xi}\nabla\Omega_{\mu\nu}\right)\left(\frac{\nabla\rho}{\xi}\nabla\Omega_{\rho\sigma}\right)d\mathbf{r} \tag{36}$$

where $\mathbf{M}$ is a general matrix, which in our case corresponds either to the $\mathbf{D}^b$ matrix given in eq 48 or to the $\mathbf{D}^f$ matrix given in eq 68. Its magnetic field derivative becomes

$$\begin{aligned}\frac{\partial G_{\mu\nu}^{xc}}{\partial B} = {}& \sum_{\rho\sigma}M_{\sigma\rho}\frac{i}{2}\int(\mathbf{R}_{MN}\times\mathbf{r})\left(\frac{\partial^2 f}{\partial\rho^2}\Omega_{\mu\nu}\Omega_{\rho\sigma} + \frac{\partial^2 f}{\partial\rho\partial\xi}\Omega_{\mu\nu}\left(\frac{\nabla\rho}{\xi}\nabla\Omega_{\rho\sigma}\right) + \frac{\partial^2 f}{\partial\rho\partial\xi}\left(\frac{\nabla\rho}{\xi}\nabla\Omega_{\mu\nu}\right)\Omega_{\rho\sigma} + \frac{\partial^2 f}{\partial\xi^2}\left(\frac{\nabla\rho}{\xi}\nabla\Omega_{\mu\nu}\right)\left(\frac{\nabla\rho}{\xi}\nabla\Omega_{\rho\sigma}\right)\right)d\mathbf{r} + \sum_{\rho\sigma}M_{\sigma\rho}\frac{i}{2}\times\\ &\int(\mathbf{R}_{RS}\times\mathbf{r})\left(\frac{\partial^2 f}{\partial\rho^2}\Omega_{\mu\nu}\Omega_{\rho\sigma} + \frac{\partial^2 f}{\partial\rho\partial\xi}\Omega_{\rho\sigma}\left(\frac{\nabla\rho}{\xi}\nabla\Omega_{\mu\nu}\right) + \frac{\partial^2 f}{\partial\rho\partial\xi}\left(\frac{\nabla\rho}{\xi}\nabla\Omega_{\rho\sigma}\right)\Omega_{\mu\nu} + \frac{\partial^2 f}{\partial\xi^2}\left(\frac{\nabla\rho}{\xi}\nabla\Omega_{\mu\nu}\right)\left(\frac{\nabla\rho}{\xi}\nabla\Omega_{\rho\sigma}\right)\right)d\mathbf{r} + \\ &\sum_{\rho\sigma}M_{\sigma\rho}\frac{i}{2}\int\left(\mathbf{R}_{MN}\times\nabla\rho(\mathbf{r})\right)\left(\frac{\partial^2 f}{\partial\rho\partial\xi}\frac{1}{\xi}\Omega_{\mu\nu}\Omega_{\rho\sigma} + \frac{\partial^2 f}{\partial\xi\partial\xi}\frac{1}{\xi^2}\Omega_{\mu\nu}(\nabla\rho\nabla\Omega_{\rho\sigma})\right)d\mathbf{r} + \sum_{\rho\sigma}M_{\sigma\rho}\frac{i}{2}\int(\mathbf{R}_{RS}\times\nabla\rho(\mathbf{r}))\times\\ &\left(\frac{\partial^2 f}{\partial\rho\partial\xi}\frac{1}{\xi}\Omega_{\mu\nu}\Omega_{\rho\sigma} + \frac{\partial^2 f}{\partial\xi^2}\frac{1}{\xi^2}\Omega_{\rho\sigma}(\nabla\rho\nabla\Omega_{\mu\nu})\right)d\mathbf{r} + G_{\mu\nu}^{xc}\left(\frac{\partial\mathbf{M}}{\partial\mathbf{B}}\right)\end{aligned} \tag{37}$$

The last term is straightforwardly obtained and is therefore not explicitly given. For the details on the derivation of the above equations, see Appendix B.

2.4. Lagrangian Approach. Having introduced all key ingredients, we can now exploit the Lagrangian approach to derive efficient computational expressions for the two quantities of interest. We will illustrate the procedure for each property separately.

2.4.1. Lagrangian Formulation of the Verdet Constant. To derive a computational expression of the Verdet constant, the Lagrangian functional is built

$$\mathscr{L}^V = \boldsymbol{A}^{[1]\dagger}\boldsymbol{b}^\omega - \bar{\boldsymbol{\lambda}}^\dagger[(\boldsymbol{E}^{[2]} - \omega\boldsymbol{S}^{[2]})\boldsymbol{b}^\omega - \boldsymbol{B}^{[1]}] - \bar{\boldsymbol{X}}^\dagger\boldsymbol{E}^{[1]} \tag{38}$$

from the linear response function in the AO basis,[74] eq 7, plus two sets of constraint equations, each multiplied with appropriate Lagrange multipliers. The constraint equations are the equations for the linear response vectors, eq 8, and the optimization condition for the "orbital" parameters **X** in the exponential parametrization of the density matrix.

$$\boldsymbol{E}^{[1]} = \mathbf{FDS} - \mathbf{SDF} = 0 \tag{39}$$

$\bar{\boldsymbol{\lambda}}^\dagger$ and $\bar{\boldsymbol{X}}^\dagger$ are referred to as the property and orbital Lagrange multipliers, respectively.

Imposing that the functional is variational with respect to all parameters, that is,

$$\frac{\partial\mathscr{L}^V}{\partial\zeta_i} = 0; \qquad \forall\zeta_i \in \{b_i^\omega, \bar{\lambda}_i, \bar{X}_i, X_i\} \tag{40}$$

yields the response equations that need to be solved, in accordance to the $2n + 1$ and $2n + 2$ rules. Differentiation with respect to all $\bar{\lambda}_i$ returns the response equation for the response vectors $\boldsymbol{b}^{\omega\omega}$ (eq 8); differentiation with respect to all $\bar{X}_i$ returns the orbital optimization condition (eq 39); differentiation with respect to b_i^ω gives the response equation that determines the multipliers $\bar{\lambda}_i$, which is in the form of an adjoint response equation

$$[(\boldsymbol{E}^{[2]} - \omega\boldsymbol{S}^{[2]})\bar{\boldsymbol{\lambda}}]^\dagger = [\boldsymbol{A}^{[1]}]^\dagger \tag{41}$$

We may therefore in the following write $\bar{\lambda} = \boldsymbol{a}^\omega$ to stress the similarity between $\bar{\lambda}$ and $\boldsymbol{b}^\omega$. Differentiation of $\mathscr{L}^V$ with respect to the (nonredundant) orbital parameters X_i gives the response equation to determine the multipliers $\bar{\boldsymbol{X}}$, which can be recast in the form

$$\boldsymbol{E}^{[2]}\bar{\boldsymbol{X}} = \eta \tag{42}$$

where the right-hand-side vector η is given by

$$\eta = \boldsymbol{A}^{[2]}\boldsymbol{b}^\omega - \boldsymbol{a}^{\omega\dagger}\boldsymbol{E}^{[3]}\boldsymbol{b}^\omega + \omega\boldsymbol{a}^{\omega\dagger}\boldsymbol{S}^{[3]}\boldsymbol{b}^\omega + \boldsymbol{B}^{[2]}\boldsymbol{a}^\omega \tag{43}$$

where the explicit expressions for the (super)matrices $\boldsymbol{A}^{[2]}$, $\boldsymbol{E}^{[3]}$, $\boldsymbol{S}^{[3]}$, and $\boldsymbol{B}^{[2]}$ may be found by differentiating with respect to the variational parameters X_i the lower order matrices ($\boldsymbol{A}^{[1]}$, $\boldsymbol{E}^{[2]}$, ...), using the rule

$$\frac{\partial\mathbf{D}(\mathbf{X})}{\partial X_j} = -[\mathbf{O}_j, \mathbf{D}]_\mathbf{S} \tag{44}$$

which stems from the exponential parametrization of the density in eq 20.[86] These matrices are also collected in Table 1.

In terms of the AO matrices that constitute the building blocks of our computational procedure, the right-hand-side matrix (in the AO space) becomes

$$\eta = -[[\mathbf{S}, \mathbf{A}]_\mathbf{b}, \mathbf{S}]_\mathbf{D} + \mathbf{KDS} - \mathbf{SDK} + \omega\mathbf{S}[\mathbf{D}, [\mathbf{a}, \mathbf{b}^\dagger]_\mathbf{s}]_\mathbf{s} + [[\mathbf{S}, \mathbf{B}^\dagger]_\mathbf{a}, \mathbf{S}]_\mathbf{D} \tag{45}$$

with

$$\mathbf{K} = [\mathbf{S}, [\mathbf{F}, \mathbf{S}]_\mathbf{a}]_{\mathbf{b}^\dagger} + [\mathbf{S}, \mathbf{G}([\mathbf{a}, \mathbf{D}])_\mathbf{S}]_{\mathbf{b}^\dagger} + [\mathbf{S}, \mathbf{G}([\mathbf{b}^\dagger, \mathbf{D}]_\mathbf{S})]_\mathbf{a} + \mathbf{G}([[\mathbf{b}^\dagger, \mathbf{D}]_\mathbf{S}, \mathbf{a}]_\mathbf{S}) \tag{46}$$

where, for ease of notation, $\mathbf{a} \equiv \mathbf{a}^\omega$ and $\mathbf{b} \equiv \mathbf{b}^\omega$. Note that because of the structure of eq 42, also the response equation determining the orbital Lagrange multipliers can be solved using the iterative response solver of ref 74 with a modified right-hand-side.

Once the response vectors have been found the computation expression for the Verdet constant is obtained from the magnetic field derivative of the Lagrangian function

$$\frac{\mathrm{d}\mathscr{L}^V}{\mathrm{d}B_\gamma} = \boldsymbol{A}^{[1],\gamma\dagger}\boldsymbol{b}^\omega - \bar{\boldsymbol{\lambda}}^\dagger[(\boldsymbol{E}^{[2],\gamma} - \omega\boldsymbol{S}^{[2],\gamma})\boldsymbol{b}^\omega - \boldsymbol{B}^{[1],\gamma}] - \bar{\boldsymbol{X}}^\dagger\boldsymbol{E}^{[1],\gamma} \tag{47}$$

The $(2n + 1)$ and $(2n + 2)$ rules allow us to neglect the dependence on the magnetic field of the parameters (e.g., response vectors and Lagrange multipliers), whereas all other matrices in the Lagrangian depend on the magnetic field through the perturbation dependent basis set (i.e., the LAOs), and the explicit dependence on the magnetic field interaction in the perturbed Hamiltonian entering the Fock/Kohn−Sham matrix **F** (hence $\boldsymbol{E}^{[2]}$ (see previous sections)). The explicit expressions for magnetic differentiated quantities are listed in Table 2.

Introducing the "perturbed" density matrices

$$\mathbf{D}^b = [\mathbf{b}, \mathbf{D}]_\mathbf{s} \tag{48}$$

$$\mathbf{D}^a = [\mathbf{D}, \mathbf{a}^\dagger]_\mathbf{s} \tag{49}$$

$$\mathbf{D}^{ab} = [[\mathbf{b}, \mathbf{D}]_\mathbf{s}, \mathbf{a}^\dagger]_\mathbf{s} + [\mathbf{D}, \bar{\mathbf{X}}^\dagger]_\mathbf{s} \tag{50}$$

the final expression for the derivative of the linear response function with respect to the magnetic field in terms of the fundamental building blocks can be written

$$\begin{aligned}\frac{\mathrm{d}\mathscr{L}^V}{\mathrm{d}B_\gamma} \equiv \frac{\mathrm{d}\alpha_{\alpha\beta}}{\mathrm{d}B_\gamma} = \mathrm{Tr}\{&\mathbf{D}^{ab}\mathbf{h}^\gamma + \mathbf{D}^{ab}\mathbf{G}^\gamma(\mathbf{D}) + \mathbf{G}^\gamma(\mathbf{D}^b)\mathbf{D}^a - \\ &\mathbf{b}[\mathbf{S}, \mathbf{A}^\gamma]_\mathbf{D} - \mathbf{b}[\mathbf{S}, \mathbf{A}]_{\mathbf{D}^\gamma} - \mathbf{b}[\mathbf{S}^\gamma, \mathbf{A}]_\mathbf{D} - \mathbf{a}^\dagger[\mathbf{S}, \mathbf{B}^\gamma]_\mathbf{D} - \\ &\mathbf{a}^\dagger[\mathbf{S}^\gamma, \mathbf{B}]_\mathbf{D} - \mathbf{a}^\dagger[\mathbf{S}, \mathbf{B}]_{\mathbf{D}^\gamma} - [\mathbf{D}, \bar{\mathbf{X}}^\dagger]_{\mathbf{S}^\gamma}\mathbf{F} - [[\mathbf{b}, \mathbf{D}]_{\mathbf{S}^\gamma}, \mathbf{a}^\dagger]_\mathbf{S}\mathbf{F} - \\ &[\mathbf{D}^b, \mathbf{a}^\dagger]_{\mathbf{S}^\gamma}\mathbf{F} - [\mathbf{D}, \mathbf{a}^\dagger]_{\mathbf{S}^\gamma}\mathbf{G}(\mathbf{D}^b) - [\mathbf{b}, \mathbf{D}]_{\mathbf{S}^\gamma}\mathbf{G}(\mathbf{D}^a) - \\ &\omega(\mathbf{a}^\dagger\mathbf{S}[\mathbf{b}, \mathbf{D}]_{\mathbf{S}^\gamma}\mathbf{S} + \mathbf{a}^\dagger\mathbf{S}^\gamma\mathbf{D}^b\mathbf{S} + \mathbf{a}^\dagger\mathbf{S}\mathbf{D}^b\mathbf{S}^\gamma) - \mathbf{D}^\gamma\mathbf{G}(\mathbf{D}^{ab}) - \\ &[\mathbf{D}^\gamma, \bar{\mathbf{X}}^\dagger]_\mathbf{S}\mathbf{F} - [[\mathbf{b}, \mathbf{D}^\gamma]_\mathbf{S}, \mathbf{a}^\dagger]_\mathbf{S}\mathbf{F} - [\mathbf{D}^\gamma, \mathbf{a}^\dagger]_\mathbf{S}\mathbf{G}(\mathbf{D}^b) - \\ &[\mathbf{b}, \mathbf{D}^\gamma]_\mathbf{S}\mathbf{G}(\mathbf{D}^a) - \omega\mathbf{a}^\dagger\mathbf{S}[\mathbf{b}, \mathbf{D}^\gamma]_\mathbf{S}\}\end{aligned} \tag{51}$$

where $\mathbf{D}^\gamma = -\mathbf{D}\mathbf{S}^\gamma\mathbf{D}$,[87] and $\mathbf{S}^\gamma$ is the magnetic field derivative (in the γ direction) of the overlap matrix.

2.4.2. Standard Quadratic-Response Formulation of the Verdet Constant. If the LAO basis is not used eq 51 reduces to the simple expression

$$\begin{aligned}\frac{\mathrm{d}\mathscr{L}^V}{\mathrm{d}B_\gamma} &= \mathrm{Tr}\{\mathbf{D}^{ab}\mathbf{h}^\gamma\} \\ &= \mathrm{Tr}\{[[\mathbf{b}, \mathbf{D}]_\mathbf{s}, \mathbf{a}^\dagger]_\mathbf{s}\mathbf{h}^\gamma\} + \mathrm{Tr}\{[\mathbf{D}, \bar{\mathbf{X}}^\dagger]_\mathbf{s}\mathbf{h}^\gamma\}\end{aligned} \tag{52}$$

Table 2. Explicit Expressions for Magnetic Differentiated Quantities

$\mathbf{E}_{[1],\gamma}$	=	$[\mathbf{S}^\gamma,\mathbf{F}]_D + [\mathbf{S},\mathbf{F}^\gamma]_D + [\mathbf{S},\mathbf{F}]_{D^\gamma}$
$\mathbf{E}_{[2],\gamma\mathbf{b}}$	=	$[\mathbf{F}^\gamma,\mathbf{S}]_{[\mathbf{b}^T,D]S} + [\mathbf{F},\mathbf{S}^\gamma]_{[\mathbf{b}^T,D]S} + [\mathbf{F},\mathbf{S}]_{[\mathbf{b}^T,D^\gamma]S} + [\mathbf{F},\mathbf{S}]_{[\mathbf{b}^T,D]S^\gamma}$
	+	$[\mathbf{G}^{\gamma,T}([\mathbf{D},\mathbf{b}]_S),\mathbf{S}]_D + [\mathbf{G}^T([\mathbf{D}^\gamma,\mathbf{b}]_S),\mathbf{S}]_D + [\mathbf{G}^T([\mathbf{D},\mathbf{b}]_{S^\gamma}),\mathbf{S}]_D$
	+	$[\mathbf{G}^T([\mathbf{D},\mathbf{b}]_S),\mathbf{S}^\gamma]_D + [\mathbf{G}^T([\mathbf{D},\mathbf{b}]_S),\mathbf{S}]_{D^\gamma}$
$\mathbf{B}_{[1],\gamma}$	=	$[\mathbf{S}^\gamma,\mathbf{B}^T]_D + [\mathbf{S},(\mathbf{B}^\gamma)^T]_D + [\mathbf{S},\mathbf{B}^T]_{D^\gamma}$
$\mathbf{A}_{[1],\gamma}$	=	$[(\mathbf{A}^\gamma)^T,\mathbf{S}]_D + [\mathbf{A}^T,\mathbf{S}^\gamma]_D + [\mathbf{A}^T,\mathbf{S}]_{D^\gamma}$
$\mathbf{S}_{[2],\gamma b}$	=	$\mathbf{S}^\gamma[\mathbf{D},\mathbf{b}^7]_S\mathbf{S} + \mathbf{S}[\mathbf{D}^\gamma,\mathbf{b}^7]_S\mathbf{S} + \mathbf{S}[\mathbf{D},\mathbf{b}^7]_{S^\gamma}\mathbf{S} + \mathbf{S}[\mathbf{D},\mathbf{b}^7]_S\mathbf{S}^\gamma$

where $\mathbf{h}^\gamma$ is now to the magnetic moment integral matrix on conventional atomic orbitals. Introducing the notation $\hat{C} = \hat{h}^\gamma$ and the $\boldsymbol{C}^{[n]}$ matrices similarly to the $\boldsymbol{B}^{[n]}$,[75] that is, $\boldsymbol{C}^{[1]} = \mathbf{h}^\gamma\mathbf{DS} - \mathbf{SDh}^\gamma$, we can rewrite eq 52 as (in supermatrix notation)

$$\frac{\mathrm{d}\mathscr{L}^V}{\mathrm{d}B_\gamma} = \boldsymbol{a}^{\omega\dagger}\boldsymbol{C}^{[2]}\boldsymbol{b}^\omega + \bar{\boldsymbol{X}}^\dagger\boldsymbol{C}^{[1]} \tag{53}$$

and the second term of it according to

$$\begin{aligned}\bar{\boldsymbol{X}}^\dagger\boldsymbol{C}^{[1]} &= (\boldsymbol{A}^{[2]}\boldsymbol{b}^\omega - \boldsymbol{a}^{\omega\dagger}\boldsymbol{E}^{[3]}\boldsymbol{b}^\omega + \omega\boldsymbol{a}^{\omega\dagger}\boldsymbol{S}^{[3]}\boldsymbol{b}^\omega + \\ &\qquad \boldsymbol{B}^{[2]}\boldsymbol{a}^\omega)^\dagger\boldsymbol{E}^{[2]^{-1}}\boldsymbol{C}^{[1]} \\ &= (\boldsymbol{b}^{\omega\dagger}\boldsymbol{A}^{[2]} - \boldsymbol{b}^{\omega\dagger}\boldsymbol{E}^{[3]}\boldsymbol{a}^\omega + \omega\boldsymbol{b}^{\omega\dagger}\boldsymbol{S}^{[3]}\boldsymbol{a}^\omega + \\ &\qquad \boldsymbol{a}^{\omega\dagger}\boldsymbol{B}^{[2]})\boldsymbol{E}^{[2]^{-1}}\boldsymbol{C}^{[1]}\end{aligned} \tag{54}$$

Introducing the response vector $\boldsymbol{c}^0$ for the static magnetic field

$$\boldsymbol{E}^{[2]}\boldsymbol{c}^0 = \boldsymbol{C}^{[1]} \tag{55}$$

we obtain the standard expression for the quadratic response function[75]

$$\begin{aligned}\frac{\mathrm{d}\mathscr{L}^V}{\mathrm{d}B_\gamma} &= \boldsymbol{a}^{\omega\dagger}\boldsymbol{C}^{[2]}\boldsymbol{b}^\omega + \boldsymbol{b}^{\omega\dagger}\boldsymbol{A}^{[2]}\boldsymbol{c}^0 - \boldsymbol{b}^{\omega\dagger}\boldsymbol{E}^{[3]}\boldsymbol{a}^\omega\boldsymbol{c}^0 + \\ &\qquad \omega\boldsymbol{b}^{\omega\dagger}\boldsymbol{S}^{[3]}\boldsymbol{a}^\omega\boldsymbol{c}^0 + \boldsymbol{a}^{\omega\dagger}\boldsymbol{B}^{[2]}\boldsymbol{c}^0 \\ &= \langle\langle\hat{A};\hat{B},\hat{C}\rangle\rangle_{\omega,0}\end{aligned} \tag{56}$$

Equation 51 thus reduces to the standard expression obtained from conventional quadratic response. Formally, both eqs 51 and 52 follow a $n + 1$ rule (with respect to the electric field), inferior to the $2n + 1$ rule, since the Lagrangian multiplier $\bar{\boldsymbol{X}}$ is a second order quantity, depending simultaneously on both the α and β directions of the perturbing electric fields. Equation 56, as well as the method presented by Krykunov et al.,[18,19] follow the superior $2n + 1$ rule. It should be noted, however, that the Verdet constant only requires crossed terms $\alpha \neq \beta \neq \gamma$, that is, one $\bar{\boldsymbol{X}}$ vector for each direction of the perturbing magnetic field, yielding to the same number of equations to be solved as in the $2n + 1$ case. Moreover, we do not need to solve any response equation that depends on the magnetic field.

2.4.3. Lagrangian Formulation of the $\mathscr{B}$ Term. For the $\mathscr{B}$ term, the Lagrangian functional is built as

$$\mathscr{L}^{\mathscr{B}} = \boldsymbol{A}^{[1]\dagger}\boldsymbol{b}^f - \bar{\boldsymbol{\lambda}}^\dagger(\boldsymbol{E}^{[2]} - \omega_f\boldsymbol{S}^{[2]})\boldsymbol{b}^f - \bar{\omega}(\boldsymbol{b}^{f\dagger}\boldsymbol{S}^{[2]}\boldsymbol{b}^f - 1) - \bar{\boldsymbol{X}}^\dagger\boldsymbol{E}^{[1]} \tag{57}$$

that is, from the expression for the transition moment, plus three constraint equations, namely the generalized eigenvalue equation for the excited state vector $\boldsymbol{b}^f$ (eq 26), its orthonormality condition (eq 27) and the optimization condition for the variational parameters $\mathbf{X}$ (eq 39).

Imposing variationality with respect to the excitation vectors yields the equation for the "property" multipliers $\bar{\boldsymbol{\lambda}}^\dagger$ and $\bar{\omega}$

$$\frac{\partial\mathscr{L}^{\mathscr{B}}}{\partial b_j^f} = 0 \Leftrightarrow A_j^{[1]} = \bar{\lambda}_m(E_{mj}^{[2]} - \omega_f S_{mj}^{[2]}) + 2\bar{\omega}b_m^f S_{mj}^{[2]} \tag{58}$$

Equation 58 may be written in its adjoint form

$$(\boldsymbol{E}^{[2]} - \omega_f\boldsymbol{S}^{[2]})\bar{\boldsymbol{\lambda}} + 2\bar{\omega}\boldsymbol{S}^{[2]}\boldsymbol{b}^f = \boldsymbol{A}^{[1]} \tag{59}$$

and projected against $\boldsymbol{b}^{f\dagger}$ and its orthogonal complement space

$$\boldsymbol{P}^{f\dagger} = (\boldsymbol{I} - \boldsymbol{S}^{[2]}\boldsymbol{b}^f\boldsymbol{b}^{f\dagger}) \tag{60}$$

Using both $\boldsymbol{b}^{f\dagger}(\boldsymbol{E}^{[2]} - \omega_f\boldsymbol{S}^{[2]}) = 0$ and the orthonormality condition eq 27, these projections give, respectively

$$\bar{\omega} = \frac{1}{2}b_f^f A_j^{[1]} = \frac{1}{2}\boldsymbol{b}^{f\dagger}\boldsymbol{A}^{[1]} \tag{61}$$

and

$$\boldsymbol{P}^{f\dagger}((\boldsymbol{E}^{[2]} - \omega_f\boldsymbol{S}^{[2]})\bar{\boldsymbol{\lambda}}) = \boldsymbol{P}^{f\dagger}\boldsymbol{A}^{[1]} \tag{62}$$

Thus, the $b^{f\dagger}$-projected equation, eq 61, uniquely determines the $\bar{\omega}$ multiplier, whereas the $P^{f\dagger}$-projected equation, eq 62, determines the multipliers $\bar{\boldsymbol{\lambda}}$. Since $\boldsymbol{P}^{f\dagger}(\boldsymbol{E}^{[2]} - \omega_f\boldsymbol{S}^{[2]}) = (\boldsymbol{E}^{[2]} - \omega_f\boldsymbol{S}^{[2]})\boldsymbol{P}^f$, where

$$\boldsymbol{P}^f = (\boldsymbol{I} - \boldsymbol{b}^f\boldsymbol{b}^{f\dagger}\boldsymbol{S}^{[2]}) \tag{63}$$

Equation 62 may be solved as

$$\boldsymbol{P}^{f\dagger}(\boldsymbol{E}^{[2]} - \omega_f\boldsymbol{S}^{[2]})\boldsymbol{P}^f\bar{\boldsymbol{\lambda}} = \boldsymbol{P}^{f\dagger}\boldsymbol{A}^{[1]} \tag{64}$$

Since we solve the above equation using an iterative procedure where trial vectors are added in pairs,[74] some modifications have to be introduced to solve these projected equations. These modifications are described in Appendix A, and the modified preconditioned conjugated gradient method displays the same convergence properties as the standard iterative procedure presented in ref 74. Note that the authors of ref 42 face a similar problem, with a singular equation, which is solved by a more straightforward projection, since the paired structure is not exploited. Note also that the corresponding equation in ref 42 (eq 24) is solved in a form with half the dimension of eq 64. However, this is done at the expense that squared excitations are obtained by solving sets of linear equations which have the squared conditioning number of eq 64 strongly impeding the convergence of the equations.

The variational condition with respect to the (nonredundant) orbital parameters X_j results in the response equation for the orbital Lagrangian multipliers $\bar{\boldsymbol{X}}$, which is clearly still

in the form of eq 42, but with a slightly different expression for the right-hand-side vector

$$\eta = \boldsymbol{b}^{f\dagger}\boldsymbol{A}^{[2]} - \boldsymbol{a}^{\omega\dagger}\boldsymbol{E}^{[3]}\boldsymbol{b}^{f} + \omega_f \boldsymbol{a}^{\omega\dagger}\boldsymbol{S}^{[3]}\boldsymbol{b}^{f} - \bar{\omega}\boldsymbol{b}^{f\dagger}\boldsymbol{S}^{[3]}\boldsymbol{b}^{f} + \frac{\partial\bar{\omega}}{\partial \boldsymbol{X}}(\boldsymbol{b}^{f\dagger}\boldsymbol{S}^{[2]}\boldsymbol{b}^{f} - 1) = \boldsymbol{b}^{f\dagger}\boldsymbol{A}^{[2]} + \omega_f \boldsymbol{a}^{\omega\dagger}S^{[3]}b^{f} - a^{\omega\dagger}\boldsymbol{E}^{[3]}\boldsymbol{b}^{f} \quad (65)$$

Equation 65 may be expressed in terms of the AO building blocks

$$\eta = -[[\mathbf{S},\mathbf{A}]_{\mathbf{b}},\mathbf{S}]_{\mathbf{D}} + \omega_f \mathbf{S}[\mathbf{D},[\mathbf{a},\mathbf{b}^{\dagger}]_{\mathbf{S}}]_{\mathbf{S}} + \mathbf{KDS} - \mathbf{SDK} \quad (66)$$

where $\mathbf{b} = \mathbf{b}^f$, and $\mathbf{a} = P^f(\boldsymbol{\lambda})$, that is, the AO matrix form of the projected solution of linear response equation in eq 62. The matrix $\mathbf{K}$ is defined analogous to the one for the Verdet constant in eq 46, but with $\mathbf{a}$ and $\mathbf{b}$ given as above.

To obtain the $\mathscr{B}$ term we finally consider the magnetic field derivative of the Lagrangian function

$$\left.\frac{\mathrm{d}\mathscr{L}^{\mathscr{B}}}{\mathrm{d}B_\gamma}\right|_{B_\gamma=0} = \boldsymbol{A}^{[1],\gamma\dagger}\boldsymbol{b}^{f} - \bar{\boldsymbol{\lambda}}^{\dagger}(\boldsymbol{E}^{[2],\gamma} - \omega_f \boldsymbol{S}^{[2],\gamma})\boldsymbol{b}^{f} + \bar{\omega}\boldsymbol{b}^{f\dagger}\boldsymbol{S}^{[2],\gamma}\boldsymbol{b}^{f} - \bar{\boldsymbol{X}}^{\dagger}\boldsymbol{E}^{[1],\gamma} \quad (67)$$

The explicit expressions for magnetic differentiated quantities are listed in Table 2. Introducing, similar to what was done for the Verdet constant, the "perturbed" transition-density matrices

$$\mathbf{D}^{f} = [\mathbf{b}^{f},\mathbf{D}]_{\mathbf{S}} \quad (68)$$

$$\mathbf{D}^{a} = [\mathbf{D},\mathbf{a}]_{\mathbf{S}} \quad (69)$$

$$\mathbf{D}^{a,f} = [[\mathbf{b}^{f},\mathbf{D}]_{\mathbf{S}},\mathbf{a}^{\dagger}]_{\mathbf{S}} + [\mathbf{D},\bar{\mathbf{X}}^{\dagger}]_{\mathbf{S}} \quad (70)$$

(where $\mathbf{a}$ is the projected linear response vector) we write the final expression for the derivative of the dipole transition strength with respect to the magnetic field in terms of the fundamental building blocks as

$$\begin{aligned}\frac{\mathrm{d}\mathscr{L}^{\mathscr{B}}}{\mathrm{d}B_\gamma} = \mathrm{Tr}\{&\mathbf{D}^{a,f}\mathbf{h}^{\gamma} + \mathbf{D}^{a,f}\mathbf{G}^{\gamma}(\mathbf{D}) + \mathbf{G}^{\gamma}(\mathbf{D}^{f})\mathbf{D}^{a} - \\ &\mathbf{b}^{f}[\mathbf{S},\mathbf{A}^{\gamma}]_{\mathbf{D}} - \mathbf{b}^{f}[\mathbf{S},\mathbf{A}]_{\mathbf{D}^{\gamma}} - \mathbf{b}^{f}[\mathbf{S}^{\gamma},\mathbf{A}]_{\mathbf{D}} - [\mathbf{D},\bar{\mathbf{X}}^{\dagger}]_{\mathbf{S}^{\gamma}}\mathbf{F} - \\ &[[\mathbf{b}^{f},\mathbf{D}]_{\mathbf{S}^{\gamma}},\mathbf{a}^{\dagger}]_{\mathbf{S}}\mathbf{F} - [\mathbf{D}^{f},\mathbf{a}^{\dagger}]_{\mathbf{S}^{\gamma}}\mathbf{F} - [\mathbf{D},\mathbf{a}^{\dagger}]_{\mathbf{S}^{\gamma}}\mathbf{G}(\mathbf{D}^{f}) - \\ &[\mathbf{b}^{f},\mathbf{D}]_{\mathbf{S}^{\gamma}}\mathbf{G}(\mathbf{D}^{a}) - \omega_f(\mathbf{a}^{\dagger}\mathbf{S}[\mathbf{b}^{f},\mathbf{D}]_{\mathbf{S}^{\gamma}}\mathbf{S} + \mathbf{a}^{\dagger}\mathbf{S}^{\gamma}\mathbf{D}^{f}\mathbf{S} + \\ &\mathbf{a}^{\dagger}\mathbf{S}\mathbf{D}^{f}\mathbf{S}^{\gamma}) - \mathbf{D}^{\gamma}\mathbf{G}(\mathbf{D}^{a,f}) - [\mathbf{D}^{\gamma},\bar{\mathbf{X}}^{\dagger}]_{\mathbf{S}}\mathbf{F} - [[\mathbf{b}^{f},\mathbf{D}^{\gamma}]_{\mathbf{S}},\mathbf{a}^{\dagger}]_{\mathbf{S}}\mathbf{F} - \\ &[\mathbf{D}^{\gamma},\mathbf{a}^{\dagger}]_{\mathbf{S}}\mathbf{G}(\mathbf{D}^{f}) - [\mathbf{b}^{f},\mathbf{D}^{\gamma}]_{\mathbf{S}}\mathbf{G}(\mathbf{D}^{a}) - \omega_f\mathbf{a}^{\dagger}\mathbf{S}[\mathbf{b}^{f},\mathbf{D}^{\gamma}]_{\mathbf{S}} + \\ &\bar{\omega}(\mathbf{b}^{f\dagger}\mathbf{S}[\mathbf{b}^{f},\mathbf{D}]_{\mathbf{S}^{\gamma}}\mathbf{S} + \mathbf{b}^{f\dagger}\mathbf{S}^{\gamma}\mathbf{D}^{f}\mathbf{S} + \mathbf{b}^{f\dagger}\mathbf{S}\mathbf{D}^{f}\mathbf{S}^{\gamma} + \mathbf{b}^{f\dagger}\mathbf{S}[\mathbf{b}^{f},\mathbf{D}^{\gamma}]_{\mathbf{S}})\}\end{aligned} \quad (71)$$

where $\bar{\omega}$, which was defined in eq 61, and is computed as

$$\bar{\omega} = \frac{1}{2}\mathrm{Tr}\{\mathbf{b}^{f}[\mathbf{A},\mathbf{S}]_{\mathbf{D}}\} \quad (72)$$

If a conventional atomic orbital basis is used instead on the LAO one, the above expression simply reduces to

$$\frac{\mathrm{d}\mathscr{L}^{\mathscr{B}}}{\mathrm{d}B_\gamma} = \mathrm{Tr}\{\mathbf{D}^{a,f}\mathbf{h}^{\gamma}\} \quad (73)$$

which with methods similar to that used in section 2.4.2 can be shown to correspond to the standard expression of the Faraday $\mathscr{B}$ term calculated as the first residue of the frequency dependent quadratic response functions.[34]

3. Illustrative Results

The computational expressions for the two MOA properties have been implemented in a local, linear-scaling version of the DALTON code. The code has been used to compute Verdet constants of H_2, HF, CO, N_2O, and propane ($CH_3CH_2CH_3$) and the $\mathscr{B}$ terms of pyrimidine, pyridine, and phosphabenzene. Selected augmented correlation-consistent basis sets[88–90] were used. For the Verdet constant, calculations were performed at $\lambda = 400$ nm for all molecules except propane, for which $\lambda = 436$ has been used for a more straightforward comparison with experiment.[91,92] At the DFT level the performance of 3 functionals was investigated, namely, the local density approximation LDA in the VWN5 parametrization,[93] B3LYP,[94] and CAMB3LYP.[95,96] The results have been benchmarked against gauge-origin independent results obtained at the CCSD level using the methodology of refs 17 and 36. Experimentally derived equilibrium geometries were used for all systems except pyrimidine, pyridine, and phosphabenzene, for which we used the B3LYP/cc-pVTZ optimized structures of ref 36.

3.1. Verdet Constants. In Table 3, we report the results for the Verdet constant of H_2 obtained at the Hartree−Fock and DFT levels. H_2 is gauge-origin independent by symmetry, but it represents nontheless a system of choice as we wish to monitor the effect of using LAOs in terms of improved convergence with respect to the basis set expansion. H_2 is also a good test system to benchmark the performance of the DFT potentials because we can compare with Full Configuration Interaction results, obtained by means of the CCSD/LAO implementation of ref 17.

Another system of choice for benchmark purposes is often HF. In this case, experimental results are not available; therefore, we limit the comparison of our Hartree−Fock and DFT values, given in Table 4, with previous gauge-origin independent CCSD results obtained in our group,[17] as well as TD-DFT results reported by Ziegler and co-workers.

Our results for carbon monoxide are collected in Table 5 and compared with both experimental and TDDFT values from Krykunov et al.[19] and with CCSD values obtained in this work.

The Verdet constants for both N_2O and propane have never been studied previously at any level of theory and are given in Tables 6 and 7, respectively. Experimental and CCSD results have also been given for N_2O, whereas for propane CCSD results have not been included, since they proved to be computationally too expensive to obtain.

We start from an analysis of the convergence of the computed results, which we illustrate in Figures 1−5. In general, one would expect the LAO basis improves the

Table 3. Magnetic Gradient of the Dipole Polarizability and Verdet Constant of H_2[a]

			$\alpha^{(m)}_{yzx}$		$V(\omega) \times 10^7$ a.u.	
method	basis	$\alpha^{(m)}_{xyz}$	non-LAO	LAO	non-LAO	LAO
Hartree−Fock	aug-cc-pVDZ	3.121966	4.721819	5.018943	0.40829	0.48696
	aug-cc-pVTZ	3.67641	4.739413	4.861765	0.45592	0.464397
	aug-cc-pVQZ	3.731024	4.781345	4.802397	0.460716	0.462175
	aug-cc-pV5Z	3.736175	4.785383	4.788590	0.461174	0.461396
	aug-cc-pV6Z	3.735484	4.785099	4.785857	0.461131	0.461183
	d-aug-cc-pVDZ	3.609032	4.329553	5.464458	0.45236	0.47296
	d-aug-cc-pVTZ	3.747092	4.801706	4.802905	0.46268	0.46277
	d-aug-cc-pVQZ	3.738836	4.789761	4.788826	0.46157	0.46151
	d-aug-cc-pV5Z	3.732110	4.783864	4.787649	0.46093	0.46119
	d-aug-cc-pV6Z	3.730353	4.782889	4.787839	0.46080	0.46114
LDA	aug-cc-pVDZ	3.876146	5.502460	8.721509	0.5157	0.7389
	aug-cc-pVTZ	5.050625	6.448561	7.159842	0.6220	0.6713
	aug-cc-pVQZ	5.286503	6.640074	6.920677	0.64346	0.6629
	aug-cc-pV5Z	5.377983	6.710685	6.842713	0.65152	0.66067
	aug-cc-pV6Z	5.420837	6.743145	6.795810	0.65526	0.65891
	daug-cc-pVDZ	5.278094	6.634525	7.403487	0.64278	0.69608
	daug-cc-pVTZ	5.449331	6.773410	6.794174	0.65834	0.65978
	daug-cc-pVQZ	5.449552	6.765238	6.769265	0.65778	0.65806
	daug-cc-pV5Z	5.448720	6.763791	6.762968	0.65766	0.65760
	daug-cc-pV6Z	5.449119	6.764166	6.764389	0.65770	0.65771
B3LYP	aug-cc-pVDZ	3.383620	4.836236	7.424569	0.45248	0.63189
	aug-cc-pVTZ	4.338292	5.591631	6.063502	0.53792	0.57063
	aug-cc-pVQZ	4.511904	5.730192	5.890203	0.55355	0.56464
	aug-cc-pV5Z	4.570646	5.774623	5.838328	0.55866	0.56308
	aug-cc-pV6Z	4.592076	5.791338	5.813249	0.56056	0.56208
	daug-cc-pVDZ	4.446419	5.665185	6.543317	0.54677	0.60764
	daug-cc-pVTZ	4.603829	5.810628	5.826199	0.56231	0.56339
	daug-cc-pVQZ	4.605892	5.803541	5.804439	0.56189	0.56195
	daug-cc-pV5Z	4.603208	5.800324	5.799311	0.56157	0.56150
	daug-cc-pV6Z	4.601501	5.798986	5.799814	0.56142	0.56148

[a] Frequency $\omega = 0.11391$ a.u. FCI/aug-cc-pV6Z: 0.45565×10^{-7} a.u. (non-LAO); 0.45578×10^{-7} a.u. (LAO)[17] Experiment: 0.501×10^{-7} a.u.[92]

Table 4. Magnetic Gradient of the Dipole Polarizability and Verdet Constant of Hydrogen Fluoride[a]

			$\alpha^{(m)}_{yzx}$		$V(\omega) \times 10^7$ a.u.	
method	basis	$\alpha^{(m)}_{xyz}$	non-LAO	LAO	non-LAO	LAO
Hartree−Fock	aug-cc-pVDZ	1.5042	1.6310	2.1578	0.16518	0.20169
	aug-cc-pVTZ	1.7011	1.8510	2.2167	0.18725	0.21260
	aug-cc-pVQZ	1.8402	2.0249	2.2130	0.20413	0.21717
	aug-cc-pV5Z	1.9054	2.0939	2.2025	0.21117	0.21870
	d-aug-cc-pVDZ	1.9379	2.1908	2.1591	0.21901	0.21683
	d-aug-cc-pVTZ	1.9782	2.1751	2.1644	0.21932	0.21857
	d-aug-cc-pVQZ	1.9802	2.1753	2.1729	0.21940	0.21924
	d-aug-cc-pV5Z	1.9794	2.1751	2.1740	0.21936	0.21929
LDA	aug-cc-pVDZ	3.98498	2.982455	4.185478	0.34482	0.42822
	aug-cc-pVTZ	4.116581	3.335878	4.329115	0.37389	0.44273
	aug-cc-pVQZ	4.444917	3.740532	4.448401	0.41331	0.46238
	aug-cc-pV5Z	4.64244	3.960753	4.451840	0.43542	0.46946
	d-aug-cc-pVDZ	4.89831	4.29881	4.46862	0.46772	0.47949
	d-aug-cc-pVTZ	5.01883	4.29655	4.312476	0.47174	0.47285
	d-aug-cc-pVQZ	5.03779	4.345523	4.345219	0.47580	0.47578
	d-aug-cc-pV5Z	5.03777	4.353641	4.352530	0.47636	0.47628
B3LYP	aug-cc-pVDZ	3.254867	2.660440	3.674269	0.29721	0.36748
	aug-cc-pVTZ	3.396116	2.948357	3.779644	0.32206	0.37968
	aug-cc-pVQZ	3.629149	3.261189	3.831202	0.35182	0.39133
	aug-cc-pV5Z	3.782167	3.435562	3.816149	0.36921	0.39559
	d-aug-cc-pVDZ	3.971842	3.706431	3.804644	0.39456	0.40136
	d-aug-cc-pVTZ	4.071619	3.701163	3.709247	0.39765	0.39821
	d-aug-cc-pVQZ	4.071138	3.727312	3.724679	0.39945	0.39902
	d-aug-cc-pV5Z	4.072300	3.732808	3.729654	0.39986	0.39965

[a] Frequency $\omega = 0.11391$ a.u. Origin on H. CCSD/aug-cc-pVTZ: 0.26473×10^{-7} a.u. (non-LAO); 0.30883×10^{-7} a.u. (LAO)[17] CCSD/d-aug-cc-pVTZ: 0.31936×10^{-7} a.u. (non-LAO); 0.32126×10^{-7} a.u. (LAO)[17] LDA/ET3/LAO: 0.53030×10^{-7} a.u.; SAOP/ET3/LAO: 0.30134×10^{-7} a.u.[19]

convergence of the results because the orbitals are correct to first order in the applied magnetic field. Indeed, the differences, when increasing the cardinal number from X = D to higher X, are significantly smaller when using the LAO basis for all methods/functionals considered, than when using conventional basis sets. The aug-cc-pVTZ/LAO basis stands out as a reasonable compromise between accuracy and computational cost. Double augmentation clearly makes the usage of LAO somewhat unnecessary, especially for $X \geq 3$; on the other hand, one would seldom use a doubly augmented basis set for large systems, since they often results in linear dependences and numerical

Table 5. Magnetic Gradient of the Dipole Polarizability and Verdet Constant of Carbon Monoxide[a]

			$\alpha^{(m)}_{yzx}$		$V(\omega) \times 10^7$ a.u.	
method	basis	$\alpha^{(m)}_{xyz}$	non-LAO	LAO	non-LAO	LAO
Hartree−Fock	aug-cc-pVDZ	11.055792	3.616679	4.273038	0.63384	0.67934
	aug-cc-pVTZ	11.406121	4.246722	4.424964	0.68965	0.70201
	aug-cc-pVQZ	11.522226	4.436302	4.471400	0.70682	0.70925
	aug-cc-pV5Z	11.546578	4.464267	4.486325	0.70960	0.71113
	daug-cc-pVDZ	11.472916	4.441526	4.374207	0.70547	0.70081
	daug-cc-pVTZ	11.529756	4.485288	4.474452	0.71047	0.70972
	daug-cc-pVQZ	11.553393	4.490153	4.489820	0.71163	0.71161
	daug-cc-pV5Z	11.556813	4.487931	4.486967	0.71159	0.71153
LDA	aug-cc-pVDZ	15.983420	6.836289	7.693072	1.02778	1.08716
	aug-cc-pVTZ	16.423412	7.438752	7.699148	1.08447	1.10283
	aug-cc-pVQZ	16.603980	7.679665	7.754938	1.10774	1.11296
	aug-cc-pV5Z	16.644201	7.726884	7.770670	1.11240	1.11545
B3LYP	aug-cc-pVDZ	13.936334	5.943637	6.815239	0.89496	0.95537
	aug-cc-pVTZ	14.414739	6.587390	6.869864	0.95616	0.97574
	aug-cc-pVQZ	14.583939	6.834959	6.915444	0.97918	0.98476
	aug-cc-pV5Z	14.621654	6.886413	6.931134	0.98406	0.98717
	daug-cc-pVDZ	14.501710	6.931655	6.867495	0.98304	0.97859
	daug-cc-pVTZ	14.614166	6.934587	6.926226	0.98714	0.98656
	daug-cc-pVQZ	14.644941	6.941044	6.942348	0.98865	0.98874
	daug-cc-pV5Z	14.644213	6.940722	6.938852	0.98860	0.98847
CAMB3LYP	aug-cc-pVDZ	13.553915	5.530387	6.423219	0.85306	0.91495
	aug-cc-pVTZ	14.034989	6.194255	6.475651	0.91575	0.93525
	aug-cc-pVQZ	14.206308	6.519579	6.448183	0.93929	0.94423
	aug-cc-pV5Z	14.244126	6.497478	6.536160	0.94402	0.94670

[a] Frequency $\omega = 0.11391$ a.u. Gauge-origin on C atom. CCSD/aug-cc-pVTZ: 0.83141×10^{-7} a.u. (non-LAO); 0.85749×10^{-7} a.u. (LAO) CCSD/aug-cc-pVQZ: 0.83560×10^{-7} a.u. (non-LAO); 0.85122×10^{-7} a.u. (LAO)LDA/ET3(LAO): 1.083409×10^{-7} a.u.[19] SAOP/ET3(LAO): 0.9156984×10^{-7} a.u.[19] Experiment: 0.895×10^{-7} a.u.[92]

Table 6. Magnetic Gradient of the Dipole Polarizability and Verdet Constant of Nitrous Oxide, N_2O[a]

			$\alpha^{(m)}_{yzx}$		$V(\omega) \times 10^7$ a.u.	
method	basis	$\alpha^{(m)}_{xyz}$	non-LAO	LAO	non-LAO	LAO
Hartree−Fock	aug-cc-pVDZ	5.20186	3.34222	5.72895	0.41193	0.57737
	aug-cc-pVTZ	5.75131	4.61477	5.36470	0.51919	0.57117
	aug-cc-pVQZ	5.99701	5.01297	5.18182	0.55530	0.56701
	aug-cc-pV5Z	6.05247	5.08413	5.16840	0.56216	0.56800
LDA	aug-cc-pVDZ	7.46008	2.26474	5.75498	0.41552	0.65744
	aug-cc-pVTZ	8.02973	3.72087	5.01409	0.53619	0.62583
	aug-cc-pVQZ	8.37503	4.24664	4.68324	0.58460	0.61486
	aug-cc-pV5Z	8.469322	4.391367	4.619600	0.59790	0.61372
B3LYP	aug-cc-pVDZ	6.945838	2.406820	5.866543	0.40754	0.64735
	aug-cc-pVTZ	7.484019	3.831389	5.168035	0.52494	0.61758
	aug-cc-pVQZ	7.835584	4.382733	4.828869	0.57567	0.60625
	aug-cc-pV5Z	7.939933	4.537069	4.755828	0.58965	0.60481
CAMB3LYP	aug-cc-pVDZ	6.749242	2.439556	5.668062	0.402998	0.62678
	aug-cc-pVTZ	7.254741	3.871418	5.038626	0.519765	0.60067
	aug-cc-pVQZ	7.593739	4.407516	4.743719	0.568672	0.59198

[a] Frequency 0.11391 a.u. Gauge-origin on the O atom. CCSD/aug-cc-pVQZ: 0.47258×10^{-7} a.u. (non-LAO); 0.54402×10^{-7} a.u. (LAO) Experiment: 0.596×10^{-7} a.u.[92]

Table 7. Magnetic Gradient of the Dipole Polarizability and Verdet Constant of Propane[a]

		$\varepsilon_{\alpha\beta\gamma}\alpha^{(m)}_{\alpha\beta\gamma}$		$V(\omega) \times 10^7$ a.u.	
method	basis	non-LAO	LAO	non-LAO	LAO
Hartree−Fock	aug-cc-pVDZ	107.493	114.951	1.7089	1.8274
	aug-cc-pVTZ	113.752	115.109	1.8083	1.8299
	aug-cc-pVQZ	114.873	115.300	1.8262	1.8330
	d-aug-cc-pVDZ	115.287	115.947	1.8328	1.8432
	d-aug-cc-pVTZ	115.494	115.506	1.8360	1.8362
LDA	aug-cc-pVDZ	149.344	167.233	2.3742	2.6585
	aug-cc-pVTZ	162.149	166.731	2.5777	2.6506
	aug-cc-pVQZ	165.502	167.411	2.6310	2.6614
	d-aug-cc-pVDZ	168.806	170.105	2.6836	2.7042
	d-aug-cc-pVTZ	168.255	168.259	2.6748	2.6749
B3LYP	aug-cc-pVDZ	132.217	147.596	2.1019	2.3258
	aug-cc-pVTZ	143.360	146.686	2.2790	2.3319
	aug-cc-pVQZ	145.816	147.166	2.3181	2.3396

[a] Wavelength 436 nm. Origin at the center of mass. Experiment: 2.34×10^{-7} a.u.[92]

instabilities, in all such cases the LAO basis stands as an effective choice to improve the convergence.

The other advantage of using the LAO basis is the gauge-origin independence of the results for any choice of basis

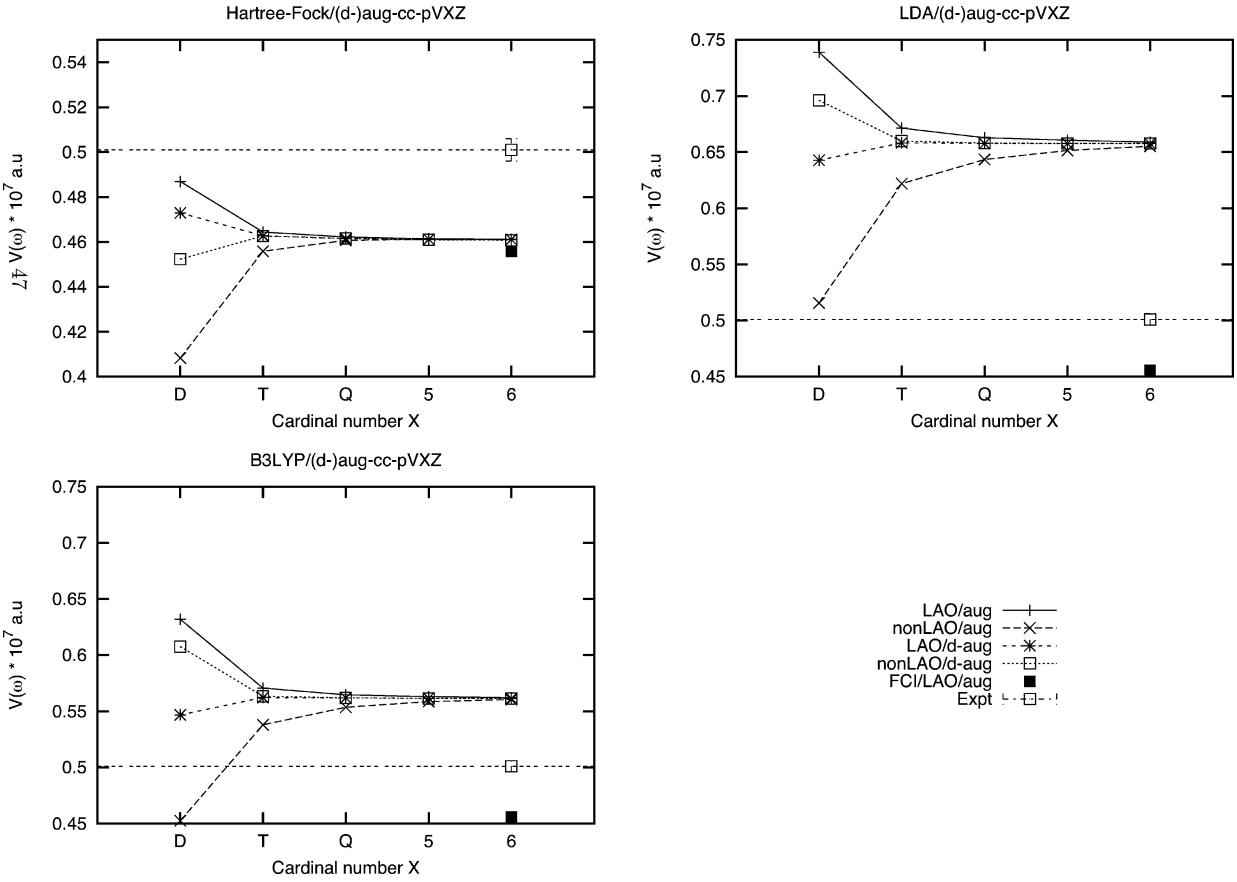

Figure 1. H2: Convergence of the Verdet constant with the basis set.

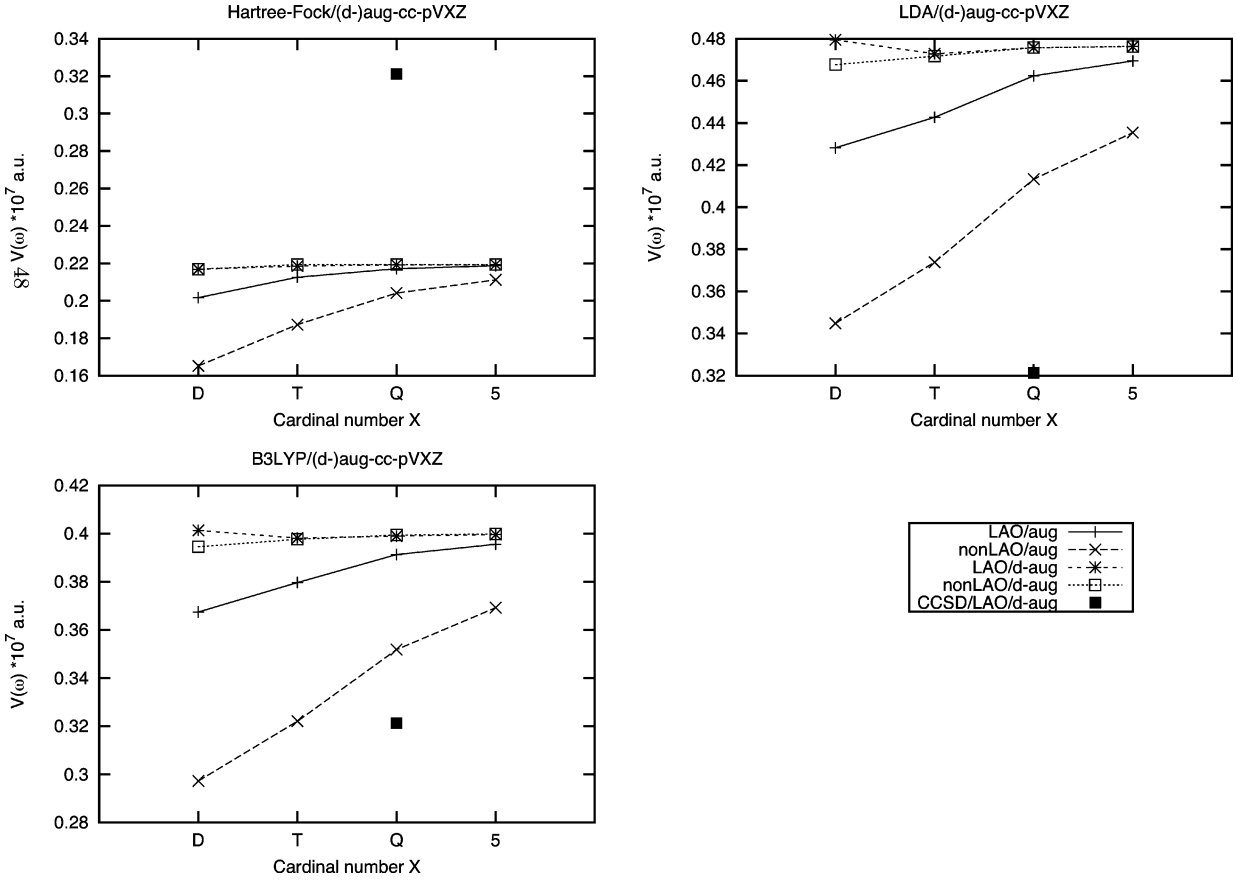

Figure 2. HF: Convergence of the Verdet constant with the basis set.

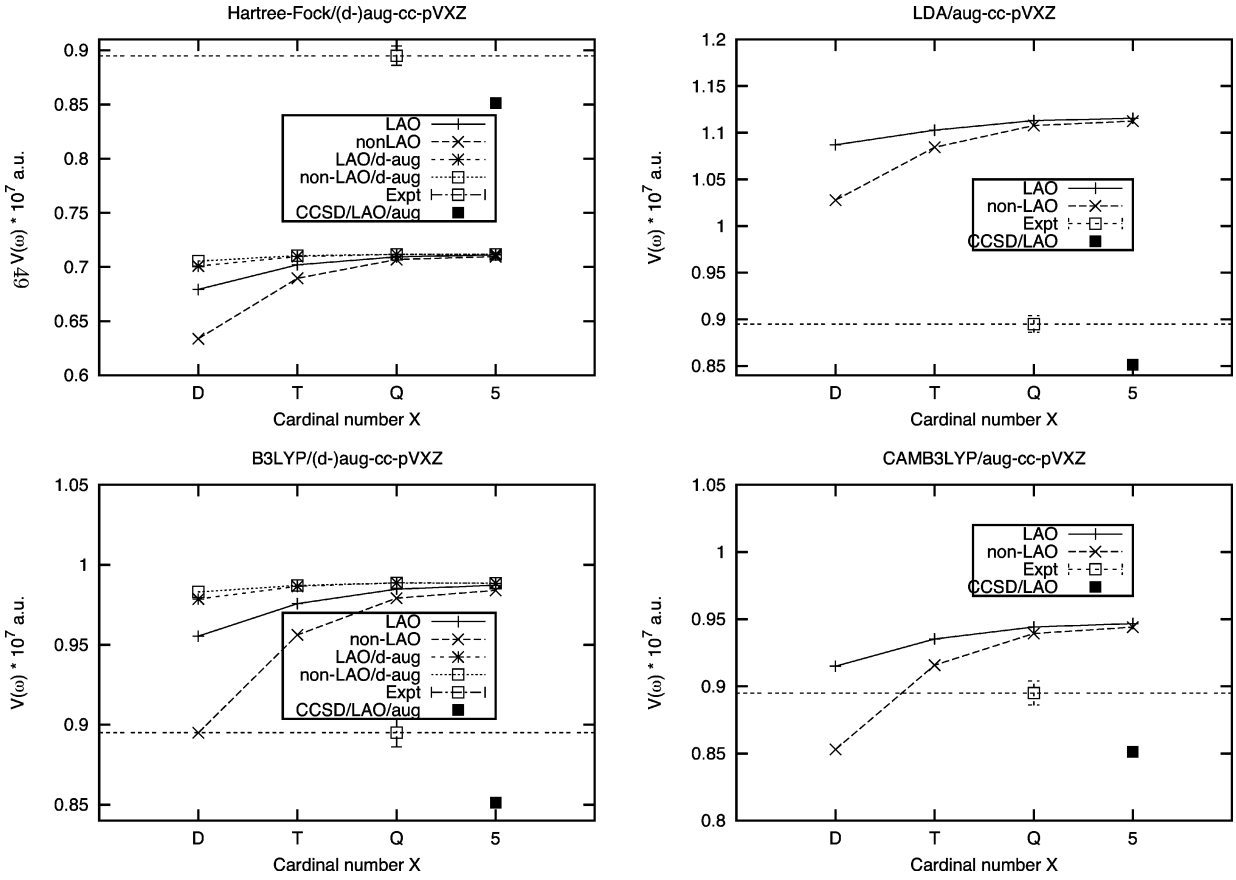

Figure 3. CO: Convergence of the Verdet constant with the basis set.

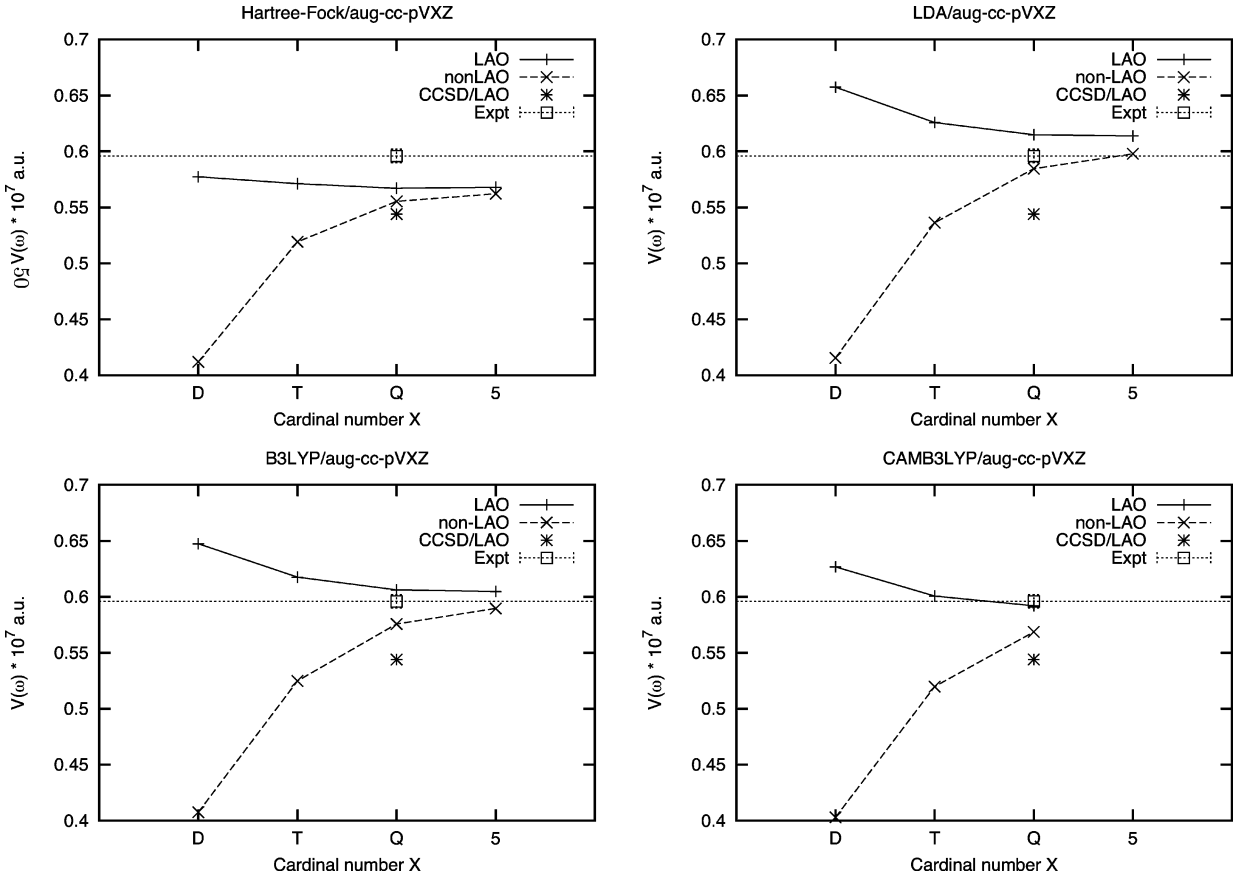

Figure 4. N_2O: Convergence of the Verdet constant with the basis set.

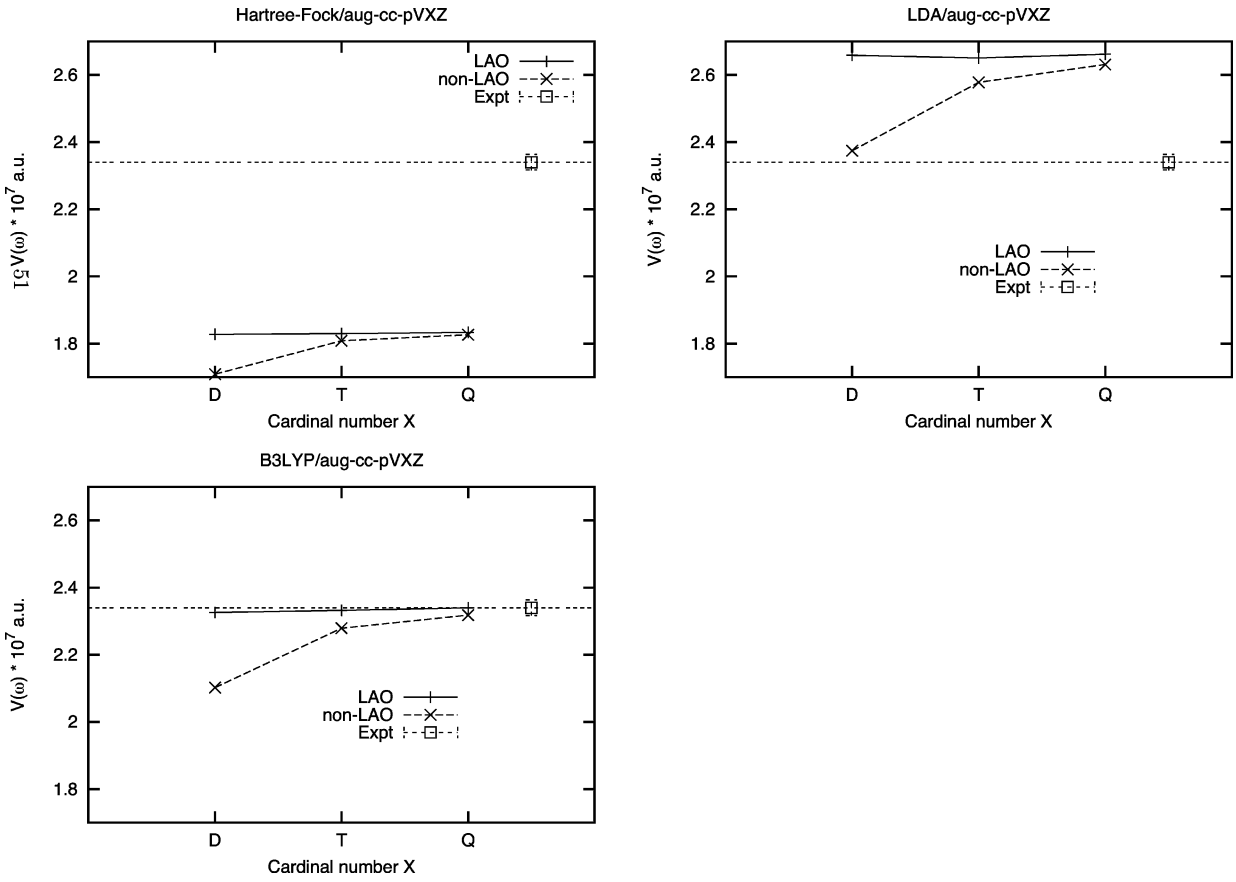

Figure 5. Propane: Convergence of the Verdet constant with the basis set.

set. The dependence of the results upon a shift of the origin of the coordinate system can, in the conventional basis set, be expressed as the difference between the value obtained at a given origin and the one obtained shifting the origin to a different point. Such difference can be written as product of the shift vector with an appropriate response function,[49] and it is expected to diminish when enlarging the basis set. We have estimated the gauge origin dependence of the results for CO, N_2O, and propane when using conventional (AO) basis sets by performing a few calculation at two different origins for each system. The overall gauge origin dependence effect was found to be rather modest with a reasonable choice of origin (below 1%) but it can be expected to become larger for extended systems.

Comparing with the experimental results at wavelengths according to refs 91 and 92, for which the authors claim an accuracy of 1%, and with our CCSD and previous DFT results from the literature, we notice that (i) For H_2 all DFT functionals here considered significantly overestimate the Verdet constant, both with respect to the benchmark FCI value, and the experimental value.[91,92] The Hartree−Fock/LAO results are, as previously observed for conventional basis sets,[15] rather close to the FCI results. The difference between experimental and FCI results can be attributed to the neglect of ro-vibrational averaging, which is of the order of 10%.[97,98] (ii) For HF, the Hartree−Fock result is well below the CCSD value, whereas both LDA and B3LYP results are larger. Our LDA results are smaller than the LDA/ET3(LAO) ones by Krykunov and co-workers.[19] (iii) The Verdet constant of CO is understimated by the Hartree−Fock method and overestimated by all DFT functionals, as also observed by Krykunov and co-workers.[19] The CCSD results are, on the other hand, always smaller than the experimental value. None of the methods, including CCSD, yields results that fall within the 1% accuracy of the experimental value (notice that no ro-vibrational averaging has been performed but the vibrational contribution is of the order of 1%.)[98] This is also in line with previous findings, like, for instance, for N_2, C_2H_2 and CH_4.[16] (iv) In N_2O all methods, apart from LDA/LAO tend to underestimate the Verdet constant. All methods also give Verdet constants that are higher than the CCSD values. The latter are, as in the previous cases, smaller than the experimental values. Also in this case all methods yield Verdet constants, which are outside the error bars of the experimental value (again neglecting ro-vibrational averaging), but to a much lesser extent than what was observed for CO. (v) In the case of propane, Hartree−Fock is once more yielding Verdet constants which are too low and outside the 1% experimental accuracy, whereas LDA results are too high. The B3LYP results, on the other hand, fall within the 1% experimental accuracy range, despite the neglect of vibrational contribution. Mort and Autschbach showed that larger molecules like benzene, toluene, *p*-xylene, and *o*-xylene also have a sizable vibrational contribution and the vibrational contribution must be taken into account for high accuracy calculations of the Verdet constant.

3.2. $\mathcal{B}$ Terms of Pyrimidine, Pyridine, and Phosphabenzene. The MCD spectra of pyrimidine, pyridine and phosphabenzene were the subject of a recent investigation at the CCSD/LAO level carried out in our group.[36] It was there

Table 8. Pyrimidine: Excitation Energies ω_f (eV), Oscillator Strengths f, and $\mathscr{B}$ Terms (10^{-3} $D^2\mu_B$ cm) for the First 5 Dipole-Allowed Electronic (Singlet) Transitions from the Ground State[a]

				$\mathscr{B}(0 \rightarrow f)$	
method/basis	symmetry	ω_f	f	non-LAO	LAO
Hartree−Fock/aug-cc-pVDZ	1 B_1	5.739	0.0072	−0.105	−0.102
	1 B_2	6.175	0.0837	1.732	1.751
	1 A_1	6.508	0.0234	−1.877	−1.895
	2 B_1	7.364	0.0241	−0.042	−0.072
	2 A_1	7.980	0.5536	5.79	5.91
LDA(VWN5)/aug-cc-pVDZ	1 B_1	3.668	0.0034	−0.050	−0.049
	2 B_1	5.155	0.0045	−0.0057	−0.0047
	1 B_2	5.551	0.0002	0.0140	0.0132
	2 B_2	5.599	0.0300	0.3087	0.3143
	1 A_1	6.219	0.0076	−0.806	−1.866
B3LYP/aug-cc-pVDZ	1 B_1	4.259	0.0046	−0.058	−0.057
	1 B_2	5.732	0.0399	0.539	0.544
	2 B_1	5.959	0.0049	−0.104	−0.101
	2 B_2	6.154	0.0006	0.0138	0.0138
	1 A_1	6.516	0.0318	−0.656	−0.657
B3LYP/aug-cc-pVTZ	1 B_1	4.2584	0.0045	−0.057	−0.057
	1 B_2	5.7240	0.0408	0.550	0.551
	2 B_1	5.9563	0.0048	−0.100	−0.099
	2 B_2	6.1562	0.0007	0.0151	0.0152
	1 A_1	6.4981	0.0311	−0.667	−0.664
CAMB3LYP/aug-cc-pVDZ	1 B_1	4.548	0.0054	−0.0670	−0.0654
	1 B_2	5.799	0.0455	0.522	0.528
	2 B_1	6.301	0.0057	−0.0717	−0.0688
	1 A_1	6.651	0.0419	−0.866	−0.872
	2 B_2	6.836	0.0044	0.0284	0.0275
CCSD/aug-cc-pVDZ-CM[36]	1 B_1	4.64	0.006		−0.068
	1 B_2	5.51	0.028		0.210
	2 B_1	6.51	0.006		−0.055
	2 B_2	6.68	0.008		0.017
	1 A_1	6.98	0.027		−0.267
experiment[99]	1 B_1	4.22	0.007		−0.06
	1 B_2	5.21	0.03		0.2
experiment[63]	1 B_1	4.29	0.0073		−0.076
	1 B_2	5.17	0.033		0.24

[a] Comparison of Hartree-Fock, LDA, B3LYP, CAMB3LYP and CCSD results. The molecule lies on the *yz* plane, with the C_2 symmetry axis along *z*.

noticed how for nonovelapping bands (e.g., for pyrimidine) the $\mathscr{B}$ terms calculated at the CCSD(/LAO) level are in good agreement with the corresponding experimental values, whereas for overlapping bands (as seen, e.g., for pyridine and phosphabenzene) significant cancellation effects between positive and negative contributions may occur, which results in a reduced magnitude of the experimentally derived $\mathscr{B}$ terms as well as in a shift of the MCD peak maxima compared to the position of the peak maxima in the UV spectrum from which the excitation energies are usually derived. Note that the MCD spectra of pyridine and pyrimidine were also very recently investigated at the DFT level by Seth et al.[42]

In Table 8, we collect the results for the excitation energies, oscillator strengths and $\mathscr{B}$ terms of MCD relative to the first 5 dipole-allowed transitions of pyrimidine obtained at the Hartree−Fock and DFT level, together with the CCSD/LAO results from reference 36, and experimental results from references 63 and 69. Analogous results are collected in Table 9 for phosphabenzene and Table 10 for pyridine.

For all three molecules, a rather small difference between LAO and AO results for the $\mathscr{B}$ terms is observed, at least for the transition considered here. Another general observation is the modest basis set effect for the low lying states (first 3−4 excitations), as it can be seen comparing the results for both excitation energies, oscillator strengths, and $\mathscr{B}$ terms obtained using the aug-cc-pVTZ basis instead of the aug-cc-pVDZ in pyrimidine (see Table 8) and phosphabenzene (see Table 9). Such small differences hardly affect the qualitative (and quantitative) features of the simulated spectra (see below). Because of the increased Rydberg character of the higher excited states, both the effect of an increased basis set and the effect of using London orbitals are more pronounced.

3.2.1. Pyrimidine. For pyrimidine, the first dipole-allowed excited state is assigned as B_1 by all methods, in accordance with the experimental assignment, but far too high in energy in the Hartree−Fock case and too low for LDA. The second state is assigned as B_2 by most methods, with the sole exception of LDA which yields a B_1 state. All methods yield negative $\mathscr{B}$ terms for all states of B_1 symmetry, as well as the first state of A_1 symmetry, and positive $\mathscr{B}$ terms for the states of B_2 symmetry, yet with magnitudes that vary significantly from method to method. Following the methodology adopted in ref 36, we show in Figure 6 the simulated MCD spectrum of pyrimidine obtained by associating to each vertical excitation energy and $\mathscr{B}$ term, obtained using the CAMB3LYP (left panel) and the B3LYP (right panel) functionals, a Gaussian line shape function and convoluting over the entire frequency region. The CCSD curve is also plotted, together with a simulated experimental spectrum (labeled Expt.) constructed from the experimentally derived $\mathscr{B}$ terms from ref 99. As it can be observed both DFT functionals display the correct qualitative features, but the absolute intensity differs significantly compared to both the CCSD values and experiment, with quite strong signals for the second

Table 9. Phosphabenzene: Excitation Energies ω_f (eV), Oscillator Strengths f, and $\mathscr{B}$ Terms (10^{-3} D$^2\mu$B cm) for the First 6 Dipole-Allowed Electronic (Singlet) Transitions from the Ground State[a]

				$\mathscr{B}(0 \rightarrow f)$	
method/basis	symmetry	ω_f	f	non-LAO	LAO
Hartree−Fock/aug-cc-pVDZ	1 A_1	4.845	0.1048	1.017	1.029
	1 B_2	5.105	0.0018	−0.979	−0.981
	1 B_1	5.708	0.0214	0.0796	0.0782
	2 B_1	6.274	0.0070	0.0674	0.0923
	2 B_2	6.343	0.3149	3.588	3.615
	2 A_1	6.810	0.6114	−2.512	−2.977
LDA(VWN5)/aug-cc-pVDZ	1 B_1	4.520	0.0148	−0.237	−0.240
	1 B_2	4.597	0.0010	0.292	0.296
	1 A_1	5.061	0.1223	0.312	0.316
	2 B_1	5.848	0.0011	−0.001	−0.007
	2 B_2	5.860	0.2242	1.964	2.060
	2 A_1	6.056	0.1223	−0.0014	−0.036
B3LYP/aug-cc-pVDZ	1 B_2	4.728	0.0008	0.359	0.361
	1 B_1	4.873	0.0173	−0.655	−0.656
	1 A_1	5.051	0.1311	0.711	0.724
	2 B_1	5.803	0.0012	0.0098	0.0128
	2 B_2	5.932	0.2465	1.996	2.020
	2 A_1	6.425	0.3042	−1.121	−1.332
B3LYP/aug-cc-pVTZ	1 B_2	4.707	0.0012	0.475	0.474
	1 B_1	4.867	0.0170	−0.771	−0.778
	1 A_1	5.016	0.1291	0.676	0.685
	2 B_1	5.776	0.0015	0.0159	0.0176
	2 B_2	5.891	0.2363	2.026	2.022
	2 A_1	6.392	0.3331	−1.676	−2.087
CAMB3LYP/aug-cc-pVDZ	1 B_2	4.825	0.0018	0.7085	0.7122
	1 B_1	5.058	0.0194	−3.342	−3.337
	1 A_1	5.098	0.1419	2.970	2.973
	2 B_2	6.052	0.2671	2.231	2.259
	2 B_1	6.206	0.0031	0.0174	0.0259
	2 A_1	6.581	0.4558	−1.390	−1.436
CCSD/aug-cc-pVDZ-CM[36]	1 B_2	4.55	0.001		0.157
	1 B_1	5.16	0.019		−0.438
	1 A_1	5.46	0.163		0.735
	2 B_1	6.18	0.005		0.042
	2 B_2	6.36	0.259		2.351
	2 A_1	6.78	0.343		−4.795
experiment[100]	1 B_2	4.22			0.11
	1 B_1	4.71			−0.10
	1 A_1	5.21	0.16		0.56

[a] Comparison of Hartree-Fock, LDA, B3LYP, CAMB3LYP and CCSD results. The molecule lies on the *yz* plane, with the C_2 symmetry axis along *z*.

Table 10. Pyridine: Excitation Energies ω_f (eV), Oscillator Strengths f and $\mathscr{B}$ Terms (10^{-3} D$^2\mu_B$ cm) for the First 6 Dipole-Allowed Electronic (Singlet) Transitions from the Ground State[a]

				$\mathscr{B}(0 \rightarrow f)$	
method/basis	symmetry	ω_f	f	non-LAO	LAO
B3LYP/aug-cc-pVDZ	1 B_1	4.765	0.0038	−0.0408	−0.0394
	1 B_2	5.473	0.0402	0.3810	0.3858
	1 A_1	6.162	0.0006	0.0215	0.0213
	2 A_1	6.242	0.0167	−0.6201	−0.6275
	2 B_2	6.654	0.0213	−0.7926	−0.8168
	2 B_1	6.7988	0.0317	5.764	4.470
	3 A_1	6.7997	0.0278	−5.179	−4.027
CAMB3LYP/aug-cc-pVDZ	1 B_1	5.037	0.0044	−0.0474	−0.0458
	1 B_2	5.542	0.0458	0.4037	0.4087
	1 A_1	6.358	0.0183	−0.7004	−0.7082
	2 A_1	6.869	0.0102	−0.0810	−0.0838
	2 B_1	7.226	0.0453	−0.0109	−0.6836
	2 B_2	7.295	0.4715	66.032	67.668
CCSD/aug-cc-pVDZ-CM[36]	1 B_1	5.18	0.005		−0.054
	1 B_2	5.28	0.028		0.163
	1 A_1	6.71	0.003		−0.042
	2 A_1	6.79	0.027		−0.365
	2 B_1	7.27	0.041		−1.547
	2 B_2	7.34	0.008		−2.300
experiment[99,63]	B_1	4.41	n.a.		−0.0002
	B_2	4.96	0.04/0.041		0.1/0.15

[a] Comparison of B3LYP, CAMB3LYP and CCSD results. The molecule lies on the *yz* plane, with the C_2 symmetry axis along *z*.

(and third) band. Only two bands appear within the frequency range considered in the simulated experimental spectrum.[99] Comparing our DFT results with those in ref 42, we note that none of the two hybrid functionals we

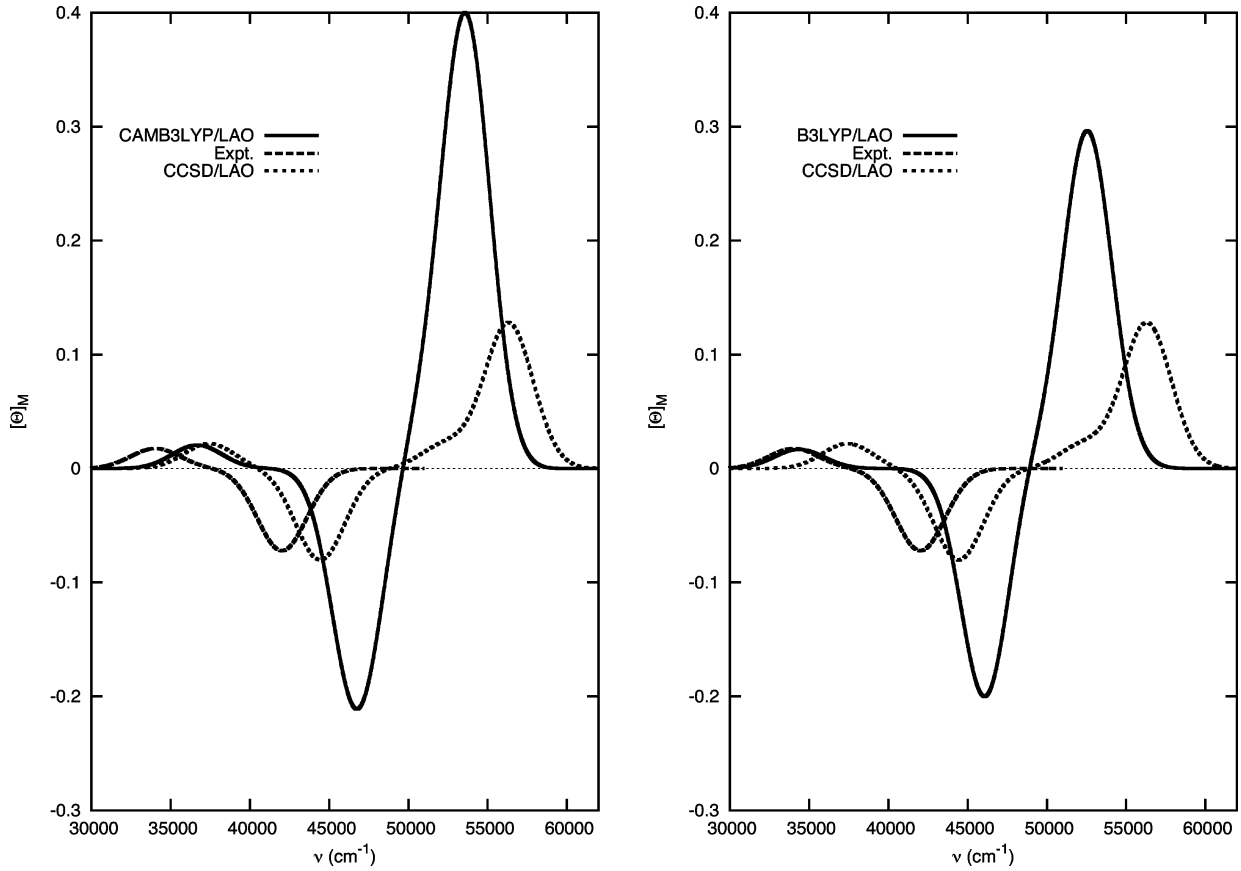

Figure 6. Pyrimidine: Comparison of simulated MCD spectra for B3LYP, CAMB3LYP, and CCSD.

have considered yields a second $n \rightarrow \pi^*$ transition of B_1 symmetry in the range 37 000−45 000 cm^{-1} as obtained instead by Seth et al. using the SAOP functional and the QZ3P1D basis set.

3.2.2. Phosphabenzene. Turning our attention to phosphabenzene, we recall that in the experimental absorption spectrum the first two transitions (assigned as B_2 and B_1) only appear as shoulders on the band for the strong transition (of A_1 symmetry) peaked at around 5.21 eV and characterized by an oscillator strength f of 0.16. The same symmetry classification is reproduced by B3LYP and CAMB3LYP (as well as CCSD), but not by Hartree−Fock and LDA. Both hybrid functionals yield $\mathscr{B}$ terms for the first three dipole-allowed transitions of the same signs as those computed by CCSD and those obtained from the experimental measurement, but again the magnitude of the terms varies significantly from method to method. This, together with the different spacing in the frequency of the various excitations yielded by the two different functionals, strongly affects the appearance of the simulated spectra reproduced in Figure 7, because of cancellation effects between bands associated with $\mathscr{B}$ terms of opposite sign falling relatively close to each other. The most remarkable consequence is the disappearance, in the B3LYP case, of the positive peak at around 40 000−42 000 cm^{-1}. As in the pyrimidine case, an estimate of the experimental spectrum from reference 100 has been included, obtained by convolution of Gaussian line shape functions built from the experimentally derived $\mathscr{B}$ terms of Waluk et al.[100]

3.2.3. Pyridine. Only B3LYP and CAMB3LYP results are reported for pyridine, together with the CCSD results from ref 36, see Table 10. Also for this molecule our previous study at the CCSD level revealed strong cancellation effects between oppositely signed MCD bands, see ref 36. Similar to what was observed for pyrimidine and phosphabenzene, the two hybrid functionals reproduce the CCSD symmetry assignment for the first four transitions (consistent with the experimental assignment for the first two transitions). Like CCSD, the two functional also yield a weaker negative $\mathscr{B}$ terms for the first transition and a stronger positive one for the second one, whereas differences are seen concerning the sign and relative intensity of the next two transitions, of A_1 symmetry. Simulating the MCD spectrum as done for the other two benzene analogues, see Figure 8, shows once again how the relative position of the excitation energy and the magnitude of the $\mathscr{B}$ terms oppositely signed dramatically affects the overall spectrum: the first positive MCD band, so weak to disappear completely in the picture at the CCSD level (in accordance to the experimental findings), is strongly enhanced at the DFT level because of the larger spacing between the first two transitions, which reduces the cancellation effect occurring between the weaker negative $\mathscr{B}$ of the first transition and the much larger positive $\mathscr{B}$ of the second transition. Similarly the second, negative, band is enhanced and the third, positive, band that dominates the DFT spectra falls at much lower frequencies than the analogous band in the CCSD spectrum. Our simulated MCD spectrum is qualitatively similar to the

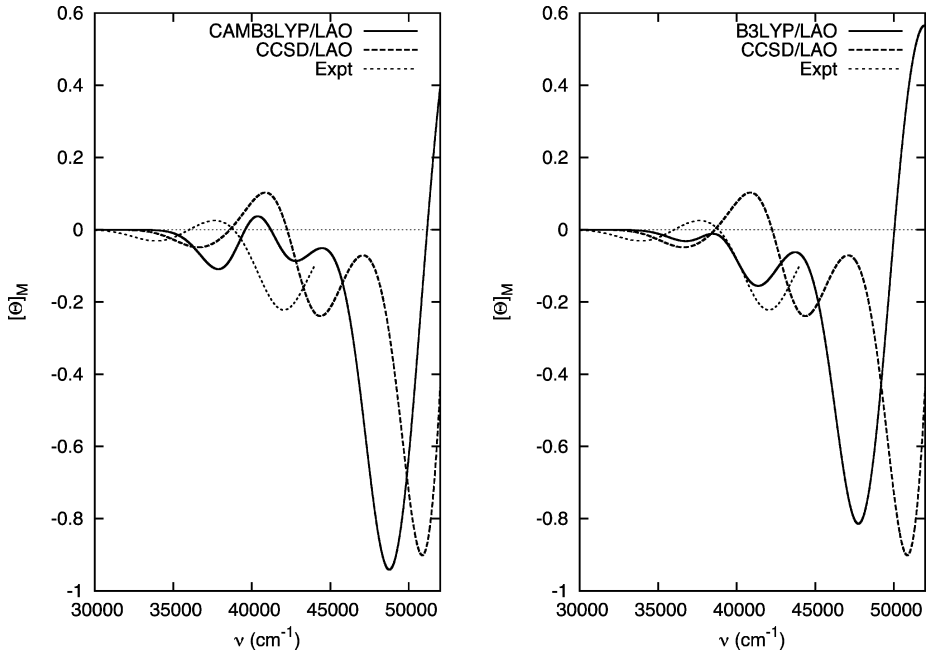

Figure 7. Phosphabenzene: Comparison of simulated MCD spectra for B3LYP, CAMB3LYP, and CCSD.

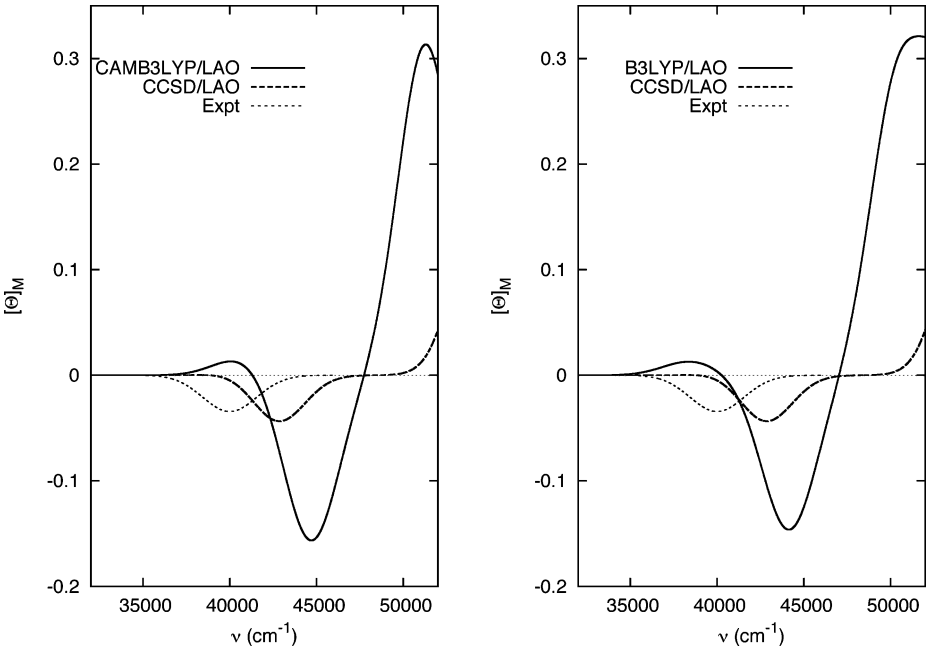

Figure 8. Pyridine: MCD spectra simulations. B3LYP/CAMB3LYP.

one obtained by Seth and co-workers in ref 42 in the frequency range of the first two dipole allowed transitions.

4. Summary and Conclusions

We have presented a Lagrangian approach to obtain gauge-origin independent expressions for the Verdet constant $V(\omega)$ of the Faraday effect and the $\mathscr{B}$ term of magnetic circular dichroism at the Hartree−Fock and TD-DFT levels of theory in an atomic-orbital based formalism suitable for linear-scaling. An important feature of the formulation is a projection to the orthogonal complement of the excited reference state to remove unphysical divergences in the response equations solved for the $\mathscr{B}$ term of MCD, and its implementation in terms of a modified preconditioned conjugated gradient method for the computation of the projected property Lagrange multipliers of the transition-moment derivative.

The methodology has been used to compute the Verdet constant of H_2, HF, CO, N_2O, and $CH_3CH_2CH_3$, as well as the $\mathscr{B}$ terms and corresponding MCD spectra of pyrimidine, phosphabenzene, and pyridine. The results have been benchmarked against CCSD values obtained applying a gauge-origin independent method previously developed in our group.[17]

Our basis set study of the Verdet constant shows that, for the functionals and molecules here considered, the model-inherent error is much larger than the basis set error, and the smallest singly augmented double-ζ basis set would

therefore suffice for qualitative comparison with experiment. Using LAOs reduces the basis set error by between 60% and 90% for singly augmented and between 0% and 50% for doubly augmented basis sets. We expect this reduction to be even greater for larger, unsymmetric molecules, where there is no obvious choice of gauge origin.

Both magneto-optical properties appear to represent quite a challenging task for both the Hartree−Fock and Kohn−Sham methods. The $\mathscr{B}$ term of MCD in particular proved very challenging, since it requires an accurate description of the excited states, the transition and the magnetic perturbation. For systems with well separated transitions the TD-DFT MCD spectra reproduce most of the qualitative features of the CCSD spectra, but information is often lost in the simulation of the MCD spectrum, especially in presence of strong overlapping bands, and the calculated $\mathscr{B}$ terms would then appear to be more useful. For the individual $\mathscr{B}$ terms, the deviation from experiment seems to lack a systematic behavior for both valence and Rydberg states, even for the CAMB3LYP functional, which has an improved long-range behavior and has been shown to better describe, compared to other functionals, excited state energies and excitations to states of Rydberg character.[101] We believe that an extensive benchmark study is required before a specific DFT functional can be recommended. In this perspective the gauge-origin-independent CCSD method of ref 17 may prove an invaluable tool for benchmarking the $\mathscr{B}$ term of MCD and determining the reliability of the $\mathscr{B}$ terms yielded by different DFT functionals. Work is in progress in this direction.

Acknowledgment. This work has received support from the Lundbeck Foundation and the Danish Center for Scientific computing. S.C. acknowledges her affiliation to the Istituto Nazionale Scienze e Tecnologia dei Materiali (INSTM) and financial support from the Italian Ministero dell'Università e Ricerca (M*i*UR), Programmi di ricerca di interesse nazionale, PRIN2006. A.J.T. has received support from the Norwegian Research Council (Grant No. 177558/V30).

Appendix

Appendix A: Modified Preconditioned Conjugated Gradient Method for the Computation of the Projected Property Lagrange Multipliers of the Transition-Moment Derivative. The variational condition of the $\mathscr{B}$-term Lagrangian with respect to the excited state vector yields a linear response equation

$$\boldsymbol{P}^{f\dagger}(\boldsymbol{E}^{[2]} - \omega_f \boldsymbol{S}^{[2]})\boldsymbol{P}^f\bar{\boldsymbol{\lambda}} = \boldsymbol{P}^{f\dagger}\boldsymbol{A}^{[1]} \tag{74}$$

where the solution vector must be orthogonal to the excitation vector using an $\boldsymbol{S}[2]$ metric, i.e. $\boldsymbol{b}^{i\dagger}\boldsymbol{S}^{[2]}\boldsymbol{b}^j = \delta_{ij}$(or $-\delta_{ij}$ for the deexcitation vectors $\boldsymbol{b}^{-i}$). The projector which ensures this orthonormality $\boldsymbol{P}^f$ is given in eq 63.

To solve eq 74, we would like to use the response solver of ref 74, which is based on an iterative preconditioned conjugate gradient algorithm (using a reduced space). Moreover the method always implicitly add trial vectors in pairs, a strategy that, for the eigenvalue problem, guarantees real eigenvalues and fast convergence.

Straightforward application of the projector $\boldsymbol{P}^f$ on the trial vector does not comply with the use of an iterative algorithm where trial vectors are added in pairs, since $\boldsymbol{b}^{-f}$ has no paired counterpart and a non-vanishing component in the solution. Thus special considerations has to be given to the $\boldsymbol{b}^{-f}$ vector when an algorithm is used where trial vectors are added in pairs.

The iterative procedure given in section II.A of ref 74 therefore has to be slightly modified when solving eq 74. The modifications may be summarized as follows:

- Instead of a basis $2n$ trial vectors (i.e., n pairs), the procedure uses a $2 + 2n$ trial vector basis, where the first two vectors are always chosen as the excitation vector $\boldsymbol{b}^f$, and its de-excitation counterpart $\boldsymbol{b}^{-f}$ ($\boldsymbol{b}^f$ and $\boldsymbol{b}^{-f}$ are the paired vectors obtained solving the eigenvalue equation, with eigenvalues ω_f and $-\omega_f$, respectively). The remaining $2n$ vectors (or n pairs) are generated (at each iteration) as in the standard procedure[74] but with the additional requirement that they are always kept orthogonal, with respect to $\boldsymbol{S}[2]$, to both $\boldsymbol{b}^f$ and $\boldsymbol{b}^{-f}$

$$\boldsymbol{b}_i = \boldsymbol{P}^{f,-f}(\boldsymbol{b}_i); \quad \forall i = 3, 2n + 2 \tag{75}$$

  The projection matrix

$$\boldsymbol{P}^{f,-f} = \boldsymbol{I} - \boldsymbol{b}^f\boldsymbol{b}^{f\dagger}\boldsymbol{S}^{[2]} + \boldsymbol{b}^{-f}\boldsymbol{b}^{-f\dagger}\boldsymbol{S}^{[2]} \tag{76}$$

  ensures this orthogonality. The $\{\boldsymbol{b}_i, i = 3, ..., 2n + 2\}$ trial vectors are, as previously, normalized and orthogonalized against each other in a standard Euclidian way, but not against the first two vectors, $\boldsymbol{b}_1 = \boldsymbol{b}^f$ and $\boldsymbol{b}_2 = \boldsymbol{b}^{-f}$.
- The above $2n + 2$ trial basis and the corresponding linear transformations $\boldsymbol{\sigma}^{2n+2}$ and $\boldsymbol{\rho}^{2n+2}$ are used to set up the response equation in a reduced space of dimension $2n + 2$. Because of the above choice of trial basis, however, the reduced space equation

$$({}^R\boldsymbol{E}^{[2]} - {}^R\omega_f {}^R\boldsymbol{S}^{[2]}){}^R\boldsymbol{X} = {}^R\boldsymbol{A}^{[1]} \tag{77}$$

$$\mathscr{R}{}^R\boldsymbol{X} = {}^R\boldsymbol{A}^{[1]} \tag{78}$$

  will have the following "blocked" structure

$$\begin{pmatrix} 0 & 0 & \dots & 0 \\ 0 & \mathscr{R}_{2,2} & \dots & \mathscr{R}_{2,2n+2} \\ \vdots & \vdots & \dots & \vdots \\ 0 & \mathscr{R}_{2n+2,2} & \dots & \mathscr{R}_{2n+2,2n+2} \end{pmatrix} \begin{pmatrix} {}^RX_1 \\ {}^RX_2 \\ \vdots \\ {}^RX_{2n+2} \end{pmatrix} = \begin{pmatrix} 0 \\ \boldsymbol{b}^{-f\dagger}\boldsymbol{P}^{f\dagger}\boldsymbol{A}^{[1]} \\ \vdots \\ \boldsymbol{b}^{\dagger}_{2n+2}\boldsymbol{P}^{f\dagger}\boldsymbol{A}^{[1]} \end{pmatrix} \tag{79}$$

  The non-zero subblock of the above equation gives the reduced space solution of the projected equation, whereas the element ${}^RX_1$ (which would give the component of the solution vector along the $\boldsymbol{b}^f$ excited state vector) is manually set to zero.
- The solution of the reduced space is used to construct the current solution vector (at each iteration) $\boldsymbol{X}$ by expansion onto the trial basis

$$\boldsymbol{X} = \sum_{i=2}^{2n+2} {}^{R}X_i \boldsymbol{b}_i \tag{80}$$

that is, with no contribution from $\boldsymbol{b}^f$ but with contribution from $\boldsymbol{b}^{-f}$. The residual is then obtained in the usual way

$$\boldsymbol{R} = \boldsymbol{E}^{[2]}\boldsymbol{X} - \omega_f \boldsymbol{S}^{[2]}\boldsymbol{X} - \boldsymbol{P}^{f\dagger}\boldsymbol{A}^{[1]} \tag{81}$$

$$\boldsymbol{R} = \sum_{i=2}^{2n} {}^{R}X_i(\boldsymbol{\sigma}_i - \omega_f \boldsymbol{\rho}_i) - \boldsymbol{P}^{f\dagger}\boldsymbol{A}^{[1]} \tag{82}$$

and preconditioned according to

$$\boldsymbol{R}_P = \boldsymbol{M}^{-1}\boldsymbol{R} \tag{83}$$

where the preconditioner $\boldsymbol{M}$ is an appropriately chosen matrix. For further information on how $\boldsymbol{M}$ is chosen, see ref 74.

- The preconditioned residual is projected with respect to the $\{\boldsymbol{b}^f, \boldsymbol{b}^{-f}\}$ space as $(\boldsymbol{P}^{f,-f}\boldsymbol{R}_P)$, and a new pair of trial vectors is then obtained according to the standard procedure of ref 74 (i.e. by normalization and orthogonalization versus the previous $\{\boldsymbol{b}_3, ..., \boldsymbol{b}_{2n+2}\}$trial vectors). The new pair of trial vectors is added to the original trial basis, the reduced space is enlarged and the iterative procedure continued until convergence, that is, until the norm of the residual is smaller than a given threshold.

Appendix B: Exchange-Correlation Contribution to the Derivative Quantities. The determination of gauge-origin independent analytic expressions for the MOA properties requires that both the derivative of the exchange-correlation contribution to the Kohn-Sham matrix $(\partial\mathbf{F}^{XC})/(\partial\boldsymbol{B})|_{\boldsymbol{B}=0}$ and the derivative of the exchange correlation contribution to the (generalized) Kohn-Sham Hessian $(\partial\mathbf{G}^{XC})/(\partial\boldsymbol{B})|_{\boldsymbol{B}=0}$ are evaluated. The object of this Appendix is to derive equations for both these exchange-correlation derivative contributions.

B.1. Exchange-Correlation Contribution to the Derivative Kohn−Sham Matrix. The exchange-correlation energy requires the integration over all space of some functional $f = f[\rho,\nabla\rho]$ which depends on the electron density $\rho = \rho(\mathbf{r})$ and on the gradient of the density $\nabla\rho = \nabla\rho(\mathbf{r})$

$$E_{xc} = \int f[\rho, \nabla\rho]d\mathbf{r} \tag{84}$$

The exchange-correlation contribution to the Kohn−Sham matrix is given by

$$F^{xc}_{\mu\nu} = \int v_{xc}\Omega_{\mu\nu}(\mathbf{r})d\mathbf{r} \tag{85}$$

where v_{xc} is the exchange correlation potential given in eq 18. Using the form of E_{xc} in eq 84 gives[102,103]

$$v_{xc} = \frac{\delta E_{xc}}{\delta\rho} = \frac{\partial f[\rho,\nabla\rho]}{\partial\rho} - \nabla\frac{\partial f[\rho,\nabla\rho]}{\partial\nabla\rho} \tag{86}$$

To simplify the evaluation of eq 85, we insert eq 86 and carry out a partial integration assuming that the constant term vanishes because f is local

$$F^{xc}_{\mu\nu} = \int \frac{\partial f}{\partial\rho}\Omega_{\mu\nu}(\mathbf{r})d\mathbf{r} + \int \frac{\partial f}{\partial\nabla\rho}\nabla\Omega_{\mu\nu}(\mathbf{r})d\mathbf{r} \tag{87}$$

Considering $\xi = |\nabla\rho|$ as the fundamental variable and applying the chain rule gives

$$F^{xc}_{\mu\nu} = \int \frac{\partial f}{\partial\rho}\Omega_{\mu\nu}(\mathbf{r})d\mathbf{r} + \int \frac{\partial f}{\partial\xi}\frac{\partial\xi}{\partial\nabla\rho}\nabla\Omega_{\mu\nu}(\mathbf{r})d\mathbf{r} \tag{88}$$

From the definition of ξ, we obtain

$$\frac{\partial\xi}{\partial\nabla\rho(\mathbf{r})} = \frac{\nabla\rho(\mathbf{r})}{\xi} \tag{89}$$

which may be inserted into eq 88 giving

$$F^{xc}_{\mu\nu} = \int \frac{\partial f}{\partial\rho}\Omega_{\mu\nu}(\mathbf{r})d\mathbf{r} + \int \frac{\partial f}{\partial\xi}\frac{\nabla\rho(\mathbf{r})}{\xi}\nabla\Omega_{\mu\nu}d\mathbf{r} \tag{90}$$

The magnetic field dependence of the Kohn−Sham matrix contribution may be introduced by replacing the atomic orbitals $\chi_\mu(\mathbf{r})$ with the London orbitals $\omega_\mu(\mathbf{B},\mathbf{r})$ of eq 29. The electron density then depends explicitly on the magnetic field as

$$\rho(\mathbf{r},\mathbf{B}) = \sum_{\mu\nu} \exp\left(\frac{i}{2}\mathbf{B}\cdot\mathbf{R}_{MN}\times\mathbf{r}\right)\chi^*_\mu(\mathbf{r})\chi_\nu(\mathbf{r})D_{\nu\mu} = \sum_{\mu\nu}\tilde{\Omega}_{\mu\nu}(\mathbf{B},\mathbf{r})D_{\nu\mu} \tag{91}$$

and the exchange-correlation contribution to the Kohn−Sham matrix becomes

$$F^{xc}_{\mu\nu} = \int \frac{\partial\tilde{f}}{\partial\tilde{\rho}}\tilde{\Omega}_{\mu\nu}d\mathbf{r} + \int \frac{\partial\tilde{f}}{\partial\tilde{\xi}}\frac{\nabla\tilde{\rho}(\mathbf{r})}{\tilde{\xi}}\nabla\tilde{\Omega}_{\mu\nu}d\mathbf{r} \tag{92}$$

where tilde is used to denote the explicit magnetic field dependence. The first derivative of the density and of the gradient of the density with respect to the field at zero field is zero[85]

$$\left.\frac{\partial\rho(\mathbf{r},\mathbf{B})}{\partial\mathbf{B}}\right|_{\mathbf{B}=0} = 0 \tag{93}$$

$$\left.\frac{\partial\nabla\rho(\mathbf{r},\mathbf{B})}{\partial\mathbf{B}}\right|_{\mathbf{B}=0} = 0 \tag{94}$$

This simplifies the differentiation of the exchange-correlation contribution to the Kohn−Sham matrix yielding

$$\left.\frac{\partial F^{xc}_{\mu\nu}}{\partial\mathbf{B}}\right|_{\mathbf{B}=0} = \int \frac{\partial f}{\partial\rho}\left.\frac{\partial\tilde{\Omega}_{\mu\nu}}{\partial\mathbf{B}}\right|_{\mathbf{B}=0}d\mathbf{r} + \int \frac{\partial f}{\partial\xi}\frac{\nabla\rho}{\xi}\left.\frac{\partial\nabla\tilde{\Omega}_{\mu\nu}}{\partial\mathbf{B}}\right|_{\mathbf{B}=0}d\mathbf{r} \tag{95}$$

From the definition of the overlap distribution $\tilde{\Omega}_{\mu\nu}$, we obtain

$$\left.\frac{\partial\tilde{\Omega}_{\mu\nu}}{\partial\mathbf{B}}\right|_{\mathbf{B}=0} = \frac{i}{2}(\mathbf{R}_{MN}\times\mathbf{r})\Omega_{\mu\nu} \tag{96}$$

The first term in eq 95 therefore becomes

$$\int \frac{\partial f}{\partial\rho}\left.\frac{\partial\tilde{\Omega}_{\mu\nu}}{\partial\mathbf{B}}\right|_{\mathbf{B}=0}d\mathbf{r} = \frac{i}{2}\int(\mathbf{R}_{MN}\times\mathbf{r})\frac{\partial f}{\partial\rho}\Omega_{\mu\nu}d\mathbf{r} \tag{97}$$

To determine the second term we derive

$$\frac{\partial \omega_q^*}{\partial r_c} = \frac{\partial}{\partial r_c} \exp\left\{\frac{i}{2}\sum_{ijk} \varepsilon_{ijk} B_i (\mathbf{R}_{QO})_j r_k\right\} \chi_q^* \tag{98}$$

$$\frac{\partial \omega_q^*}{\partial r_c} = \frac{i}{2}\left(\sum_{ij} \varepsilon_{ijc} B_i (\mathbf{R}_{QO})_j\right) \exp\left\{\frac{i}{2}\sum_{ijk} \varepsilon_{ijk} B_i (R_{QO})_j r_k\right\} \chi_q^* + \exp\left\{\frac{i}{2}\sum_{ijk} \varepsilon_{ijk} B_i (\mathbf{R}_{QO})_j r_k\right\} \frac{\partial \chi_q^*}{\partial r_c} \tag{99}$$

where the Levi−Civita tensor has been introduced to describe the cross-product and c denotes a spatial electronic coordinate component. A subsequent differentiation with respect to a magnetic field yields

$$\left.\frac{\partial}{\partial B_\gamma}\frac{\partial \omega_q^*}{\partial r_c}\right|_{\boldsymbol{B}=0} = \frac{i}{2}\left(\sum_j \varepsilon_{\gamma jc} (\mathbf{R}_{QO})_j\right)\chi_q + \frac{i}{2}(\mathbf{R}_{QO} \times \mathbf{r})_\gamma \frac{\partial \chi_q}{\partial r_c} \tag{100}$$

which may be used to obtain

$$\left.\frac{\partial}{\partial B_\gamma}\frac{\partial \tilde{\Omega}_{\mu\nu}}{\partial r_c}\right|_{\boldsymbol{B}=0} = \frac{i}{2}\left(\sum_j \varepsilon_{\gamma jc} (\mathbf{R}_{MN})_j\right)\Omega_{\mu\nu} + \frac{i}{2}(\mathbf{R}_{MN} \times \mathbf{r})_\gamma \frac{\partial \Omega_{\mu\nu}}{\partial r_c} \tag{101}$$

Inserting eq 101 into the second term of eq 95 gives

$$\begin{aligned}
&\int \frac{\partial f}{\partial \xi}\frac{\nabla \rho}{\xi}\left.\frac{\partial \nabla \tilde{\Omega}_{\mu\nu}}{\partial B_\gamma}\right|_{\boldsymbol{B}=0} \mathrm{d}\mathbf{r} \\
&\quad = \int \frac{\partial f}{\partial \xi}\frac{1}{\xi}\sum_c \frac{\partial \rho}{\partial r_c}\frac{\partial}{\partial B_\gamma}\left.\frac{\partial \tilde{\Omega}_{\mu\nu}}{\partial r_c}\right|_{\mathbf{B}=0} \mathrm{d}\mathbf{r} \\
&\quad = \int \frac{\partial f}{\partial \xi}\frac{1}{\xi}\sum_{cj} \frac{\partial \rho}{\partial r_c}\frac{i}{2}(\varepsilon_{\gamma jc}(\mathbf{R}_{MN})_j)\Omega_{\mu\nu}\mathrm{d}\mathbf{r} \\
&\quad + \int \frac{\partial f}{\partial \xi}\frac{1}{\xi}\sum_c \frac{i}{2}(\mathbf{R}_{MN} \times \mathbf{r})_\gamma \frac{\partial \rho}{\partial r_c}\frac{\partial \Omega_{\mu\nu}}{\partial r_c}\mathrm{d}\mathbf{r} \\
&= \int \frac{\partial f}{\partial \xi}\frac{1}{\xi}\frac{i}{2}((\mathbf{R}_{MN} \times \nabla \rho)_\gamma \Omega_{\mu\nu} + (\mathbf{R}_{MN} \times \mathbf{r})_\gamma \nabla \rho \nabla \Omega_{\mu\nu})\mathrm{d}\mathbf{r}
\end{aligned} \tag{102}$$

The exchange-correlation contribution to the derivative Kohn−Sham matrix may therefore be obtained as

$$\left.\frac{\partial F_{\mu\nu}^{\mathrm{xc}}}{\partial B}\right|_{\boldsymbol{B}=0} = \frac{i}{2}\int (\mathbf{R}_{MN} \times \mathbf{r})\left[\frac{\partial f}{\partial \rho(\mathbf{r})}\Omega_{\mu\nu}(\mathbf{r}) + \frac{\partial f}{\partial \xi}\frac{\nabla \rho(\mathbf{r})}{\xi}\nabla \Omega_{\mu\nu}(\mathbf{r})\right]\mathrm{d}\mathbf{r} + \frac{i}{2}\int \left(\mathbf{R}_{MN} \times \frac{\nabla \rho(\mathbf{r})}{\xi}\right)\frac{\partial f}{\partial \xi}\Omega_{\mu\nu}(\mathbf{r})\mathrm{d}\mathbf{r} \tag{103}$$

where we have used eq 97 and eq 102.

B.2. Exchange-Correlation Contribution to the Derivative Generalized Kohn−Sham Hessian Matrix. The exchange-correlation contribution to the (generalized) Kohn-Sham Hessian is determined by[75]

$$G_{\mu\nu}^{\mathrm{xc}}(\mathbf{M}) = \sum_{\rho\sigma} M_{\sigma\rho}\int \frac{\delta v_{\mathrm{xc}}(\mathbf{r})}{\delta \rho(\mathbf{s})}\Omega_{\mu\nu}(\mathbf{r})\Omega_{\rho\sigma}(\mathbf{s})\mathrm{d}\mathbf{r}\mathrm{d}\mathbf{s} \tag{104}$$

where $\mathbf{M}$ is a general "perturbed" density matrix, in our case either $\mathbf{D}^b$ or $\mathbf{D}^f$. Using eq 86, we obtain

$$G_{\mu\nu}^{\mathrm{xc}}(\mathbf{M}) = \sum_{\rho\sigma} M_{\sigma\rho}\int \frac{\delta}{\delta \rho(\mathbf{s})}\frac{\partial f[\rho(\mathbf{r}), \nabla \rho(\mathbf{r})]}{\partial \rho(\mathbf{r})}\Omega_{\mu\nu}(\mathbf{r})\Omega_{\rho\sigma}(\mathbf{s})\mathrm{d}\mathbf{r}\mathrm{d}\mathbf{s} - \sum_{\rho\sigma} M_{\sigma\rho}\int \frac{\delta}{\delta \rho(\mathbf{s})}\nabla_r\left(\frac{\partial f[\rho(\mathbf{r}), \nabla \rho(\mathbf{r})]}{\partial \nabla \rho(\mathbf{r})}\right)\Omega_{\mu\nu}(\mathbf{r})\Omega_{\rho\sigma}(\mathbf{s})\mathrm{d}\mathbf{r}\mathrm{d}\mathbf{s} \tag{105}$$

where the subscript ∇_r denotes the variable with respect to which we differentiate. Using partial integration on the second term and assuming that the constant term vanishes because f is local gives

$$G_{\mu\nu}^{\mathrm{xc}}(\mathbf{M}) = \sum_{\rho\sigma} M_{\sigma\rho}\int \frac{\delta}{\delta \rho(\mathbf{s})}\frac{\partial f[\rho(\mathbf{r}), \nabla \rho(\mathbf{r})]}{\partial \rho(\mathbf{r})}\Omega_{\mu\nu}(\mathbf{r})\Omega_{\rho\sigma}(\mathbf{s})\mathrm{d}\mathbf{r}\mathrm{d}\mathbf{s} + \sum_{\rho\sigma} M_{\sigma\rho}\int \frac{\delta}{\delta \rho(\mathbf{s})}\frac{\partial f[\rho(\mathbf{r}), \nabla \rho(\mathbf{r})]}{\partial \nabla \rho(\mathbf{r})}\nabla_r(\Omega_{\mu\nu}(\mathbf{r}))\Omega_{\rho\sigma}(\mathbf{s})\mathrm{d}\mathbf{r}\mathrm{d}\mathbf{s} \tag{106}$$

Using the chain rule for functional derivatives

$$\frac{\delta F}{\delta g(y)} = \int \frac{\delta F}{\delta f(x)}\frac{\delta f(x)}{\delta g(y)}\mathrm{d}x \tag{107}$$

yields

$$G_{\mu\nu}^{\mathrm{xc}}(\mathbf{M}) = P_1 + P_2 + P_3 + P_4 \tag{108}$$

$$P_1 = \sum_{\rho\sigma} M_{\sigma\rho}\int \frac{\delta \partial f[\rho(\mathbf{r}), \nabla \rho(\mathbf{r})]}{\delta \rho(\mathbf{t})\partial \rho(\mathbf{r})}\frac{\delta \rho(\mathbf{t})}{\delta \rho(\mathbf{s})}\Omega_{\mu\nu}(\mathbf{r})\Omega_{\rho\sigma}(\mathbf{s})\mathrm{d}\mathbf{r}\mathrm{d}\mathbf{s}\mathrm{d}\mathbf{t} \tag{109}$$

$$P_2 = \sum_{\rho\sigma} M_{\sigma\rho}\int \frac{\delta \partial f[\rho(\mathbf{r}), \nabla \rho(\mathbf{r})]}{\delta \rho(\mathbf{t})\partial \nabla \rho(\mathbf{r})} \times \frac{\delta \rho(\mathbf{t})}{\delta \rho(\mathbf{s})}\nabla_r(\Omega_{\mu\nu}(\mathbf{r}))\Omega_{\rho\sigma}(\mathbf{s})\mathrm{d}\mathbf{r}\mathrm{d}\mathbf{s}\mathrm{d}\mathbf{t} \tag{110}$$

$$P_3 = \sum_{\rho\sigma} M_{\sigma\rho}\int \frac{\delta \partial f[\rho(\mathbf{r}), \nabla \rho(\mathbf{r})]}{\delta \nabla \rho(\mathbf{t})\partial \rho(\mathbf{r})} \times \frac{\delta \nabla \rho(\mathbf{t})}{\delta \rho(\mathbf{s})}\Omega_{\mu\nu}(\mathbf{r})\Omega_{\rho\sigma}(\mathbf{s})\mathrm{d}\mathbf{r}\mathrm{d}\mathbf{s}\mathrm{d}\mathbf{t} \tag{111}$$

$$P_4 = \sum_{\rho\sigma} M_{\sigma\rho}\int \frac{\delta \partial f[\rho(\mathbf{r}), \nabla \rho(\mathbf{r})]}{\delta \nabla \rho(\mathbf{t})\partial \nabla \rho(\mathbf{r})} \times \frac{\delta \nabla \rho(\mathbf{t})}{\delta \rho(\mathbf{s})}\nabla_r(\Omega_{\mu\nu}(\mathbf{r}))\Omega_{\rho\sigma}(\mathbf{s})\mathrm{d}\mathbf{r}\mathrm{d}\mathbf{s}\mathrm{d}\mathbf{t} \tag{112}$$

Using the relation between functional and standard derivatives for composite functions

$$\frac{\delta \rho(\mathbf{t})}{\delta \rho(\mathbf{s})} = \delta(\mathbf{t} - \mathbf{s}) \tag{113}$$

$$\frac{\delta f[\rho(\mathbf{r})]}{\delta \rho(\mathbf{t})} = \frac{\partial f[\rho(\mathbf{r})]}{\partial \rho(\mathbf{r})}\delta(\mathbf{r} - \mathbf{t}) \tag{114}$$

and integrating first over $\mathbf{s}$ and then $\mathbf{t}$, the first two terms of eq 108 may be rewritten

$$P_1 + P_2 = \sum_{\rho\sigma} M_{\sigma\rho}\int \frac{\partial^2 f}{\partial \rho^2}\Omega_{\mu\nu}\Omega_{\rho\sigma}\mathrm{d}\mathbf{r} + \sum_{\rho\sigma} M_{\sigma\rho}\int \frac{\partial^2 f}{\partial \rho \partial \nabla \rho}\nabla(\Omega_{\mu\nu})\Omega_{\rho\sigma}\mathrm{d}\mathbf{r} \tag{115}$$

Using the relation

$$\frac{\delta\nabla\rho(\mathbf{t})}{\delta\rho(\mathbf{s})} = \nabla_t\frac{\delta\rho(\mathbf{t})}{\delta\rho(\mathbf{s})} = \nabla_t\delta(\mathbf{t}-\mathbf{s}) \tag{116}$$

the last two terms become

$$\begin{aligned} P_3 + P_4 = &\sum_{\rho\sigma} M_{\sigma\rho}\int \frac{\delta\partial f[\rho(\mathbf{r}),\nabla\rho(\mathbf{r})]}{\delta\nabla\rho(\mathbf{t})\partial\rho(\mathbf{r})}\times \\ &\nabla_t\delta(\mathbf{t}-\mathbf{s})\Omega_{\mu\nu}(\mathbf{r})\Omega_{\rho\sigma}(\mathbf{s})\mathrm{d}\mathbf{r}\mathrm{d}\mathbf{s} + \\ &\sum_{\rho\sigma} M_{\sigma\rho}\int \frac{\delta\partial f[\rho(\mathbf{r}),\nabla\rho(\mathbf{r})]}{\delta\nabla\rho(\mathbf{t})\partial\nabla\rho(\mathbf{r})}\times \\ &\nabla_t\delta(\mathbf{t}-\mathbf{s})\nabla_r(\Omega_{\mu\nu}(\mathbf{r}))\Omega_{\rho\sigma}(\mathbf{s})\mathrm{d}\mathbf{r}\mathrm{d}\mathbf{s} \end{aligned} \tag{117}$$

Performing a partial integration, assuming that the constant term vanishes because f is a local function, gives

$$\begin{aligned} P_3 + P_4 = &-\sum_{\rho\sigma} M_{\sigma\rho}\int \nabla_t\left(\frac{\delta\partial f[\rho(\mathbf{r}),\nabla\rho(\mathbf{r})]}{\delta\nabla\rho(\mathbf{t})\partial\rho(\mathbf{r})}\right)\times \\ &\delta(\mathbf{t}-\mathbf{s})\Omega_{\mu\nu}(\mathbf{r})\Omega_{\rho\sigma}(\mathbf{s})\mathrm{d}\mathbf{r}\mathrm{d}\mathbf{s}\mathrm{d}\mathbf{t} - \\ &\sum_{\rho\sigma} M_{\sigma\rho}\int \nabla_t\left(\frac{\delta\partial f[\rho(\mathbf{r}),\nabla\rho(\mathbf{r})]}{\delta\nabla\rho(\mathbf{t})\partial\nabla\rho(\mathbf{r})}\right)\times \\ &\delta(\mathbf{t}-\mathbf{s})\nabla_r(\Omega_{\mu\nu}(\mathbf{r}))\Omega_{\rho\sigma}(\mathbf{s})\mathrm{d}\mathbf{r}\mathrm{d}\mathbf{s}\mathrm{d}\mathbf{t} \end{aligned} \tag{118}$$

Performing the integration over $\mathbf{t}$ yields

$$\begin{aligned} P_3 + P_4 = &-\sum_{\rho\sigma} M_{\sigma\rho}\int \nabla_s\left(\frac{\delta\partial f[\rho(\mathbf{r}),\nabla\rho(\mathbf{r})]}{\delta\nabla\rho(\mathbf{s})\partial\rho(\mathbf{r})}\right)\times \\ &\Omega_{\mu\nu}(\mathbf{r})\Omega_{\rho\sigma}(\mathbf{s})\mathrm{d}\mathbf{r}\mathrm{d}\mathbf{s} - \sum_{\rho\sigma} M_{\sigma\rho}\int \nabla_s\left(\frac{\delta\partial f[\rho(\mathbf{r}),\nabla\rho(\mathbf{r})]}{\delta\nabla\rho(\mathbf{s})\partial\nabla\rho(\mathbf{r})}\right)\times \\ &\nabla_r(\Omega_{\mu\nu}(\mathbf{r}))\Omega_{\rho\sigma}(\mathbf{s})\mathrm{d}\mathbf{r}\mathrm{d}\mathbf{s} \end{aligned} \tag{119}$$

Yet another partial integration and an integration over $\mathbf{s}$ using eq 114 yields

$$\begin{aligned} P_3 + P_4 = &\sum_{\rho\sigma} M_{\sigma\rho}\int \frac{\partial^2 f}{\partial\rho\partial\nabla\rho}\Omega_{\mu\nu}\nabla\Omega_{\rho\sigma}\mathrm{d}\mathbf{r} + \\ &\sum_{\rho\sigma} M_{\sigma\rho}\int \frac{\partial^2 f}{\partial(\nabla\rho)^2}\nabla\Omega_{\mu\nu}\nabla\Omega_{\rho\sigma}\mathrm{d}\mathbf{r} \end{aligned} \tag{120}$$

The total $G^{\mathrm{xc}}_{\mu\nu}(\mathbf{M})$ may be obtained from eq 115 and 120 giving

$$\begin{aligned} G^{\mathrm{xc}}_{\mu\nu}(\mathbf{M}) = &\sum_{\rho\sigma} M_{\sigma\rho}\int \frac{\partial^2 f}{\partial\rho^2}\Omega_{\mu\nu}\Omega_{\rho\sigma} + \frac{\partial^2 f}{\partial\rho\partial\nabla\rho}(\Omega_{\mu\nu}\nabla\Omega_{\rho\sigma} + \\ &\Omega_{\rho\sigma}\nabla\Omega_{\mu\nu})\mathrm{d}\mathbf{r} + \sum_{\rho\sigma} M_{\sigma\rho}\int \frac{\partial^2 f}{\partial(\nabla\rho)^2}\nabla\Omega_{\mu\nu}\nabla\Omega_{\rho\sigma}\mathrm{d}\mathbf{r} \end{aligned} \tag{121}$$

The general chain rule

$$\frac{\partial f}{\partial\nabla\rho} = \frac{\partial f}{\partial\xi}\frac{\partial\xi}{\partial\nabla\rho} = \frac{\nabla\rho}{\xi} \tag{122}$$

$$\frac{\partial^2 f}{\partial(\nabla\rho)^2} = \frac{\partial^2 f}{\partial\xi^2}\left(\frac{\partial\xi}{\partial\nabla\rho}\right)^2 + \frac{\partial f}{\partial\xi}\frac{\partial^2\xi}{\partial(\nabla\rho)^2} = \frac{\partial^2 f}{\partial\xi^2}\left(\frac{\nabla\rho}{\xi}\right)^2 \tag{123}$$

can now be applied in order to introduce $\xi = |\nabla\rho|$ as the fundamental variable

$$\begin{aligned} G^{\mathrm{xc}}_{\mu\nu}(\mathbf{M}) = &\sum_{\rho\sigma} M_{\sigma\rho}\int \frac{\partial^2 f}{\partial\rho^2}\Omega_{\mu\nu}\Omega_{\rho\sigma} + \frac{\partial^2 f}{\partial\rho\partial\xi}\left(\Omega_{\mu\nu}\frac{\nabla\rho}{\xi}\nabla\Omega_{\rho\sigma} + \right. \\ &\left.\Omega_{\rho\sigma}\frac{\nabla\rho}{\xi}\nabla\Omega_{\mu\nu}\right)\mathrm{d}\mathbf{r} + \sum_{\rho\sigma} M_{\sigma\rho}\int \frac{\partial^2 f}{\partial\xi^2}\left(\frac{\nabla\rho}{\xi}\nabla\Omega_{\mu\nu}\right)\left(\frac{\nabla\rho}{\xi}\nabla\Omega_{\rho\sigma}\right)\mathrm{d}\mathbf{r} \end{aligned} \tag{124}$$

Differentiation of the $\mathbf{G}^{\mathrm{xc}}$ matrix elements eq 124 with respect to a magnetic field (at zero magnetic field strength) gives

$$\begin{aligned} \left.\frac{\partial G^{\mathrm{xc}}_{\mu\nu}(\mathbf{M})}{\partial\mathbf{B}}\right|_{\mathbf{B}=0} = &\sum_{\rho\sigma} M_{\sigma\rho}\frac{i}{2}\int(\mathbf{R}_{MN}\times\mathbf{r})\left(\frac{\partial^2 f}{\partial\rho^2}\Omega_{\mu\nu}\Omega_{\rho\sigma} + \right. \\ &\frac{\partial^2 f}{\partial\rho\partial\xi}\Omega_{\mu\nu}\left(\frac{\nabla\rho}{\xi}\nabla\Omega_{\rho\sigma}\right) + \frac{\partial^2 f}{\partial\rho\partial\xi}\left(\frac{\nabla\rho}{\xi}\nabla\Omega_{\mu\nu}\right)\Omega_{\rho\sigma} + \\ &\left.\frac{\partial^2 f}{\partial\xi^2}\left(\frac{\nabla\rho}{\xi}\nabla\Omega_{\mu\nu}\right)\left(\frac{\nabla\rho}{\xi}\nabla\Omega_{\rho\sigma}\right)\right)\mathrm{d}\mathbf{r} + \sum_{\rho\sigma} M_{\sigma\rho}\frac{i}{2}\times \\ &\int(\mathbf{R}_{RS}\times\mathbf{r})\left(\frac{\partial^2 f}{\partial\rho^2}\Omega_{\mu\nu}\Omega_{\rho\sigma} + \frac{\partial^2 f}{\partial\rho\partial\xi}\Omega_{\rho\sigma}\left(\frac{\nabla\rho}{\xi}\nabla\Omega_{\mu\nu}\right) + \right. \\ &\left.\frac{\partial^2 f}{\partial\rho\partial\xi}\left(\frac{\nabla\rho}{\xi}\nabla\Omega_{\rho\sigma}\right)\Omega_{\mu\nu} + \frac{\partial^2 f}{\partial\xi^2}\left(\frac{\nabla\rho}{\xi}\nabla\Omega_{\mu\nu}\right)\left(\frac{\nabla\rho}{\xi}\nabla\Omega_{\rho\sigma}\right)\right)\mathrm{d}\mathbf{r} + \\ &\sum_{\rho\sigma} M_{\sigma\rho}\frac{i}{2}\int(\mathbf{R}_{MN}\times\nabla\rho)\left(\frac{\partial^2 f}{\partial\rho\partial\xi}\frac{1}{\xi}\Omega_{\mu\nu}\Omega_{\rho\sigma} + \right. \\ &\left.\frac{\partial^2 f}{\partial\xi\partial\xi}\frac{1}{\xi^2}\Omega_{\mu\nu}(\nabla\rho\nabla\Omega_{\rho\sigma})\right)\mathrm{d}\mathbf{r} + \\ &\sum_{\rho\sigma} M_{\sigma\rho}\frac{i}{2}\int(\mathbf{R}_{RS}\times\nabla\rho))\left(\frac{\partial^2 f}{\partial\rho\partial\xi}\frac{1}{\xi}\Omega_{\mu\nu}\Omega_{\rho\sigma} + \right. \\ &\left.\frac{\partial^2 f}{\partial\xi^2}\frac{1}{\xi^2}\Omega_{\rho\sigma}(\nabla\rho\nabla\Omega_{\mu\nu})\right)\mathrm{d}\mathbf{r} + G^{\mathrm{xc}}_{\mu\nu}\left(\frac{\partial\mathbf{M}}{\partial\mathbf{B}}\right) \end{aligned} \tag{125}$$

where we have used eq 96 and 101 and that all contributions from differentiation of the density itself vanish due to eq 93 and 94. The last term in eq 125 can be straightforwardly derived and is therefore omitted.

References

(1) Faraday, M. *Philos. Mag.* **1846**, *28*, 294.

(2) Faraday, M. *Philos. Trans. R. Soc. London* **1846**, *136*, 1.

(3) Barron, L. D. *Molecular Light Scattering and Optical Activity*; 2nd ed. revised and enlarged; Cambridge University Press: Cambridge, England, 2004 pp 292.

(4) Caldwell, D. J.; Eyring, H. The Faraday Effect. In *The Theory of Optical Activity*; Wiley-Interscience: New York, 1971; pp 167−193.

(5) Buckingham, A. D.; Stephens, P. J. *Adv. Res. Chem. Phys.* **1966**, *17*, 399.

(6) Schatz, P. N.; McCaffery, A. J. *Q. Rev.* **1969**, *23*, 552.

(7) Sutherland, J. C. The magnetic optical activity of hemoproteins. In *The Porphyrins*; Dolphin, D., Ed.; Academic Press: New York, 1978; Vol. 1, p 56.

(8) Dawson, J. H.; Dooley, D. M. Magnetic circular dichroism spectroscopy of iron porphyrins and heme proteins. In *Iron Porphyrins*; Lever, A.; Gray, H. P., Eds.; VCH: New York, 1989; Vol 3.

(9) Gorski, A.; Vogel, E.; Sessler, J. L.; Waluk, J. *J. Phys. Chem. A* **2002**, *106*, 8139.

(10) Kobayashi, N.; Nakai, K. *Chem. Commun.* **2007**, 4077–4092.

(11) Pearce, L. L.; Bominaar, E. L.; Peterson, J. *Biochem. Biophys. Res. Commun.* **2002**, *297*, 220.

(12) Verdet, E. M. *Ann. Chim. (3rd Ser.)* **1854**, *41*, 370.

(13) Kula, M.; Cappelli, C.; Coriani, S.; Rizzo, A. *ChemPhysChem* **2008**, *9*, 462.

(14) Botek, E.; Champagne, B.; Verbiest, T.; Gangopadhyay, P.; Persoons, A. *ChemPhysChem* **2006**, *7*, 1654.

(15) Coriani, S.; Hättig, C.; Jørgensen, P.; Halkier, A.; Rizzo, A. *Chem. Phys. Lett.* **1997**, *281*, 445 Erratum, **1998**, *293*, 324.

(16) Coriani, S.; Jørgensen, P.; Christiansen, O.; Gauss, J. *Chem. Phys. Lett.* **2000**, *330*, 463.

(17) Coriani, S.; Hättig, C.; Jørgensen, P.; Helgaker, T. *J. Chem. Phys.* **2000**, *113*, 3561.

(18) Banerjee, A.; Autschbach, J.; Ziegler, T. *Int. J. Quantum Chem.* **2005**, *101*, 572.

(19) Krykunov, M.; Banerjee, A.; Ziegler, T.; Autschbach, J. *J. Chem. Phys.* **2005**, *122*, 074105.

(20) Michl, J.; Thulstrup, E. W. *Spectroscopy with Polarized Light*; VCH Publishers, Inc.: New York, 1986.

(21) Thulstrup, E. W. *Aspects of the Linear Magnetic Circular Dichroism of Planar Organic Molecules*; Springer-Verlag: Berlin, 1980.

(22) Mason, W. R. *A Practical Guide to Magnetic Circular Dichroism Spectroscopy*; John Wiley and Sons: New York, 2007.

(23) Piepho, S. B.; Schatz, P. N. *Group Theory in Spectroscopy: With Applications to Magnetic Circular Dichroism*, John Wiley and Sons: New York, 1983.

(24) Solomon, E.; Pavel, E.; Loeb, K.; Campochiaro, C. *Coord. Chem. Rev.* **1995**, *144*, 369.

(25) Kirk, M.; Peariso, K. *Curr. Opin. Chem. Biol.* **2003**, *7*, 220.

(26) Cheeseman, M.; Greenwood, C.; Thomson, T. J. *Advances in Inorganic Chemistry*; Academic Press: San Diego, CA, 1991; Vol. 36, pp 201−255.

(27) Serber, R. *Phys. Rev.* **1932**, 41.

(28) Stephens, P. J. *Chem. Phys. Lett.* **1968**, *2*, 241.

(29) Stephens, P. J. *J. Chem. Phys.* **1970**, *52*, 3489.

(30) Stephens, P. J. *Annu. Rev. Phys. Chem.* **1974**, *25*, 201.

(31) Stephens, P. J. *Adv. Chem. Phys.* **1976**, *35*, 197.

(32) Solheim, H.; Ruud, K.; Coriani, S.; Norman, P. *J. Phys. Chem. A* **2008**, *112*, 9615.

(33) Seamans, L.; Moscowitz, A. *J. Chem. Phys.* **1972**, *56*, 1099.

(34) Coriani, S.; Jørgensen, P.; Rizzo, A.; Ruud, K.; Olsen, J. *Chem. Phys. Lett.* **1999**, *300*, 61.

(35) Honda, Y.; Hada, M.; Ehara, M.; Nakatsuji, H.; Michl, J. *J. Chem. Phys.* **2005**, *123*, 164113.

(36) Kjærgaard, T.; Jansík, B.; Jørgensen, P.; Coriani, S.; Michl, J. *J. Phys. Chem. A* **2007**, *111*, 11278.

(37) Solheim, H.; Frediani, L.; Ruud, K.; Coriani, S. *Theor. Chem. Acc.* **2008**, *119*, 231.

(38) Solheim, H.; Ruud, K.; Coriani, S.; Norman, P. *J. Chem. Phys.* **2008**, *128*, 094103.

(39) Seth, M.; Ziegler, T.; Banerjee, A.; Autschbach, J.; van Gisbergen, S.; Baerends, E. *J. Chem. Phys.* **2004**, *120*, 10942.

(40) Seth, M.; Ziegler, T.; Autschbach, J. *J. Chem. Phys.* **2005**, *122*, 094112.

(41) Peralta, G. A.; Seth, M.; Ziegler, T. *J. Chem. Theory Comput.* **2007**, *3*, 434.

(42) Seth, M.; Krykunov, M.; Ziegler, T.; Autschbach, J.; Banerjee, A. *J. Chem. Phys.* **2008**, *128*, 144105.

(43) Peralta, G. A.; Seth, M.; Ziegler, T. *Inorg. Chem.* **2007**, *46*, 9111.

(44) Krykunov, M.; Seth, M.; Ziegler, T.; Autschbach, J. *J. Chem. Phys.* **2007**, *127*, 244102.

(45) Ganyushin, D.; Neese, F. *J. Chem. Phys.* **2008**, *128*, 114117.

(46) Seth, M.; Ziegler, T. *Inorg. Chem.* **2009**, *48*, 1793.

(47) Jørgensen, P.; Oddershede, J.; Beebe, N. H. F. *J. Chem. Phys.* **1978**, *68*, 2527.

(48) Jaszuński, M.; Jørgensen, P.; Rizzo, A.; Ruud, K.; Helgaker, T. *Chem. Phys. Lett.* **1994**, *222*, 263.

(49) Parkinson, W. A.; Sauer, S. P. A.; Oddershede, J.; Bishop, D. M. *J. Chem. Phys.* **1993**, *98*, 487.

(50) Jaszuński, M.; Jørgensen, P.; Rizzo, A. *Theor. Chim. Acta* **1995**, *90*, 291.

(51) Coriani, S.; Hättig, C.; Rizzo, A. *J. Chem. Phys.* **1999**, *111*, 7828.

(52) London, F. *J. Phys. Radium* **1937**, *8*, 397.

(53) Helgaker, T.; Jørgensen, P. *J. Chem. Phys.* **1991**, *95*, 2595.

(54) Bak, K. L.; Hansen, A. E.; Ruud, K.; Helgaker, T.; Olsen, J.; Jørgensen, P. *Theor. Chim. Acta* **1995**, *90*, 441.

(55) Miles, D. W.; Eyring, H. *Proc. Natl. Acad. Sci. U.S.A.* **1973**, *70*, 3754.

(56) Meier, A. R.; Wagnière, G. H. *Chem. Phys.* **1987**, *113*, 287.

(57) Shieh, D. J.; Lin, S. H.; Eyring, H. *J. Phys. Chem.* **1972**, *76*, 1844.

(58) Goldstein, E.; Vijaya, S.; Segal, G. A. *J. Am. Chem. Soc.* **1980**, *102*, 6198.

(59) Marconi, G. *Chem. Phys. Lett.* **1988**, *146*, 259.

(60) Michl, J. *Tetrahedron* **1974**, *30*, 4215.

(61) Fleischhauer, J.; Michl, J. *J. Phys. Chem. A* **2000**, *104*, 7776.

(62) Caldwell, D.; Eyring, H. *J. Chem. Phys.* **1973**, *58*, 1149.

(63) Kaito, A.; Tajiri, A.; Hatano, M. *J. Am. Chem. Soc.* **1976**, *96*, 384.

(64) Sprinkel, F. M.; Shillady, D. D.; Strickland, R. W. *J. Am. Chem. Soc.* **1975**, *97*, 6653.

(65) Seth, M.; Krykunov, M.; Ziegler, T.; Autschbach, J. *J. Chem. Phys.* **2008**, *128*, 234102.

(66) Seth, M.; Ziegler, T. *J. Chem. Phys.* **2007**, *127*, 134108.

(67) Seamans, L.; Linderberg, J. *Mol. Phys.* **1972**, *24*, 1393.

(68) Gross, E. K. U.; Dobson, J. F.; Petersilka, M. Density functional theory of time-dependent phenomena. In *Topics in Current Chemistry*; Springer: Berlin Heidelberg, 1996; Vol. 181, pp 82.

(69) van Leeuwen, R. *Int. J. Mod. Phys. B* **2001**, *15*, 1969.

(70) Koch, W.; Holthausen, M. C. A. *Chemist's Guide to Density Functional Theory*, 2nd ed.; Wiley-VCH: Weinheim, Germany, 2001.

(71) Sałuek, P.; Høst, S.; Thøgersen, L.; Jørgensen, P.; Manninen, P.; Olsen, J.; Jansík, B.; Reine, S.; Pawlowski, F.; Tellgren,

E.; Helgaker, T.; Coriani, S. *J. Chem. Phys.* **2007**, *126*, 114110.

(72) Rubensson, E. H.; Sałek, P. *J. Comput. Chem.* **2005**, *26*, 1628.

(73) Jansík, B.; Høst, S.; Jørgensen, P.; Olsen, J.; Helgaker, T. *J. Chem. Phys.* **2007**, *126*, 124104.

(74) Coriani, S.; Høst, S.; Jansík, B.; Thøgersen, L.; Olsen, J.; Jørgensen, P.; Reine, S.; Pawlowski, F.; Helgaker, T.; Sałek, P. *J. Chem. Phys.* **2007**, *126*, 154108.

(75) Kjærgaard, T.; Jørgensen, P.; Olsen, J.; Coriani, S.; Helgaker, T. *J. Chem. Phys.* **2008**, *129*, 054106.

(76) Larsen, H.; Jørgensen, P.; Olsen, J.; Helgaker, T. *J. Chem. Phys.* **2000**, *113*, 8908.

(77) Coriani, S.; Kjærgaard, T.; Jørgensen, P.; Ruud, K.; Berger, R. Unpublished work.

(78) Furche, F.; Ahlrichs, R. *J. Chem. Phys.* **2002**, *117*, 7433.

(79) Rappoport, D.; Furche, F. *J. Chem. Phys.* **2007**, *126*, 201104.

(80) Thorvaldsen, A.; Ruud, K.; Kristensen, K.; Jørgensen, P.; Coriani, S. *J. Chem. Phys.* **2008**, *129*, 214108.

(81) Shcherbin, D.; Thorvaldsen, A. J.; Ruud, K.; Coriani, S.; Rizzo, A. *Phys. Chem. Chem. Phys.* **2009**, *11*, 816.

(82) Buckingham, A. D.; Jamieson, M. J. *Mol. Phys.* **1971**, *22*, 117.

(83) Olsen, J.; Jørgensen, P. *J. Chem. Phys.* **1985**, *82*, 3235.

(84) Olsen, J.; Jørgensen, P. Time-dependent response theory with application to self-consistent field and multiconfigurational self-consistent field wave functions. In *Modern Electronic Structure Theory*, Part II; Yarkony, D. R., Ed.; World Scientific: Singapore, 1995; Vol 2, pp 857.

(85) Helgaker, T.; Wilson, P. J.; Amos, R. D.; Handy, N. C. *J. Chem. Phys.* **2000**, *113*, 2983.

(86) Helgaker, T.; Jørgensen, P.; Olsen, J. *Molecular Electronic−Structure Theory*; Wiley: Chichester, U.K., 2000; pp 468.

(87) Larsen, H.; Helgaker, T.; Jørgensen, P.; Olsen, J. *J. Chem. Phys.* **2001**, *115*, 10344.

(88) Dunning, T. H., Jr. *J. Chem. Phys.* **1989**, *90*, 1007.

(89) Woon, D. E.; Dunning, T. H., Jr. *J. Chem. Phys.* **1993**, *98*, 1358.

(90) Woon, D. E.; Dunning, T. H., Jr. *J. Chem. Phys.* **1994**, *100*, 2975.

(91) Ingersoll, L. R.; Liebenberg, D. H. *J. Opt. Soc. Am.* **1954**, *44*, 566.

(92) Ingersoll, L. R.; Liebenberg, D. H. *J. Opt. Soc. Am.* **1956**, *46*, 538.

(93) Vosko, S.; L. Wilk, L.; Nusair, M. *Can. J. Phys.* **1980**, *58*, 1200.

(94) Becke, A. D. *J. Chem. Phys.* **1993**, *98*, 5648.

(95) Yanai, T.; Tew, D. P.; Handy, N. C. *Chem. Phys. Lett.* **2004**, *393*, 51.

(96) Peach, M. J. G.; Helgaker, T.; Sałek, P.; Keal, T. W.; Lutnæs, O. B.; Tozer, D. J.; Handy, N. C. *Phys. Chem. Chem. Phys.* **2006**, *8*, 558.

(97) Bishop, D. M.; Cybulski, S. *J. Chem. Phys.* **1990**, *93*, 590.

(98) Mort, B.; Autschbach, J. *J. Phys. Chem. A* **2007**, 5563–5571.

(99) Castellan, A.; Michl, J. *J. Am. Chem. Soc.* **1978**, *100*, 6824.

(100) Waluk, J.; Klein, H.; Ashe, A. J.; Michl, J. *Organometallics* **1989**, *8*, 2804.

(101) Peach, M. J. G.; Benfield, P.; Helgaker, T.; Tozer, D. J. *J. Chem. Phys.* **2008**, *128*, 044118.

(102) Parr, R. G.; Yang, W. *Density-Functional Theory of Atoms and Molecules*; Oxford Science Publications: Oxford, U.K., 1989.

(103) Sałek, P.; Hesselmann, A. *J. Comput. Chem.* **2007**, *28*, 2569.

CT9001625